

Monte Carlo studies of phase transitions and critical phenomena

I K Kamilov, A K Murtazaev, Kh K Aliev

Contents

1. Introduction	689
2. MC methods in statistical physics	690
2.1 Classical MC method; 2.2 Quantum Monte Carlo method	
3. Studies of PT and CP in model systems	693
4. Phase transitions and critical phenomena in quantum lattice models	695
5. Studies of PT and CE in models of real magnetic substances	697
5.1 CE in small magnetic particles; 5.2 Phase transitions and critical phenomena in macrosystems; 5.3 Finite-size scaling and critical exponents of models of real magnets	
6. MC study of the dynamic critical behavior	704
7. Conclusions	706
References	707

Abstract. The current state of Monte Carlo work on phase transitions and critical phenomena is reviewed. Both classical and quantum Monte Carlo results are discussed with emphasis on statistical lattice-model studies involving the highly accurate calculation of critical exponents. It is shown that finite-size scaling is an effective method whereby not only simple lattice models but also those of complex practical magnetic materials can be treated. For models allowing crossover phenomena, it is shown that both finite-size scaling theory and conventional power-law functions must be used in carrying out a Monte Carlo analysis.

1. Introduction

In recent years we have witnessed considerable progress in the understanding of phase transitions (PT) and critical phenomena (CP), a lot of the credit for which should go to the ideas based on the scaling and universality hypotheses and the theory of renormalization group (RG) [1–4]. A precursor of these microscopic approaches is the phenomenological Landau theory of second-order phase transitions in the framework of which critical exponents (CE) were calculated for the first time. However, the numerical values of these exponents did not coincide with those obtained experimentally in magnets, ferroelectrics, and liquids. V L Ginzburg was the first to point out that spatially heterogeneous fluctuations of the order parameter should be taken into account in the

Landau theory [5]. He suggested a criterion for the applicability of the Landau theory, which was shown to be valid as long as the fluctuations of the order parameter, averaged over a volume comparable with the coherence length, are less than the order parameter. The recognition of the paramount importance of the consideration of the order parameter fluctuations has played a key role in the development of the above-mentioned microscopic theories and approaches. They have appeared a good tool to enable researchers to obtain the majority of important results of modern PT and CP theories, to reveal the main features of the behavior in the critical region, to find relations between the critical exponents and critical amplitudes (CA), to derive equations of state, and to calculate values of CE and CA. The RG method and the ε expansion are considered nowadays to yield the most precise and reliable values of CE and CA obtained by approximate methods [6–8]. The ideas underlying all these methods have provided a deep insight into the nature of critical phenomena. Nevertheless, we have to state that no rigorous microscopic theory of the second-order phase transitions still exists nowadays [9]. The majority of theoretical results that were obtained in recent years are based on the use of the RG method. But some of the statements and techniques employed in the RG theory cannot be considered rigorously proved and justified [2]. Note also that the problem of the influence of nonideal features, inherent in real systems, on the results of studying CP are still to be understood. Now the emphasis is given to the study of more realistic models with regard to numerous complicating factors, such as anisotropy and impurity effects, multispin exchange, dipole–dipole interaction, lattice vibrations, etc. inherent in real systems, but disregarded in the earlier models [2] (e.g., the classical Ising and Heisenberg models). A rigorous study of such systems with the use of microscopic Hamiltonians by methods of modern theoretical physics is an extremely difficult problem. In view of this and some other reasons, phase transitions and critical phenomena are intensively investigated by numerical-simulation methods such as Monte Carlo (MC) and molecular dynamics (MD) [10–18]. The present stage of the

I K Kamilov, A K Murtazaev Dagestan Scientific Center Institute of Physics, Russian Academy of Sciences,
ul. Yaragского 94, 367003 Makhachkala, Russian Federation
Tel. (8-8722) 62 89 60
Kh K Aliev Dagestan State University,
ul. M Gadzhieva 43a, 367025 Makhachkala, Russian Federation
Tel. (8-8722) 67 59 65

Received 1 April 1999
Uspekhi Fizicheskikh Nauk **169** (7) 773–795 (1999)
Translated by G N Chuev; edited by S N Gorin

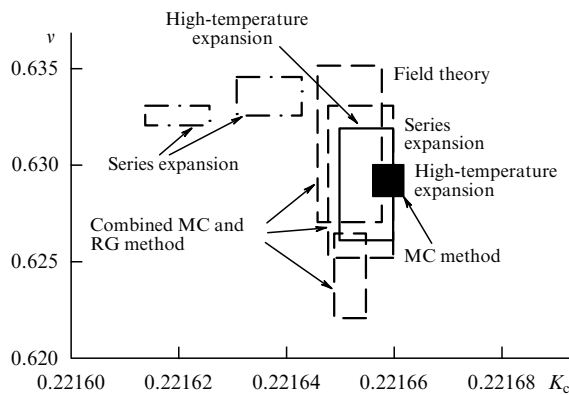


Figure 1. Values of the inverse critical temperature K_c and the critical exponent ν of correlation radius obtained within the 3d Ising model on a simple cubic lattice by various methods [146].

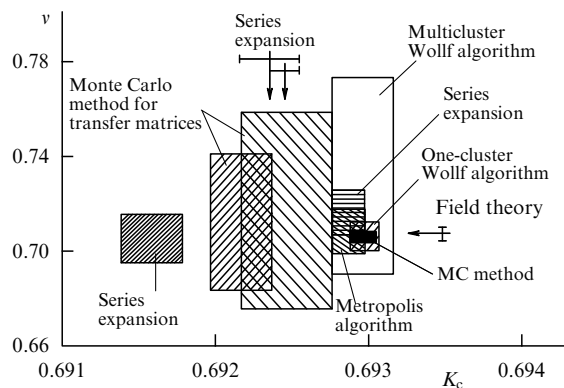


Figure 2. Values of the inverse critical temperature K_c and the critical exponent ν of correlation radius obtained within the 3d Heisenberg model on a simple cubic lattice by various methods [147].

studies of PT and CP can probably be called ‘computer-based.’ For comparison, Figs 1 and 2 show the data on the critical exponent ν of the correlation radius and the inverse critical temperature $K_c = J/k_B T$, obtained by various methods for the Ising and Heisenberg models (here and below we use the conventional symbols for the critical exponents). Although the quantitative study of the critical region by MC methods has been made possible only in the very recent past, the accuracy of the data obtained is highly competitive with the most accurate results obtained by other methods and sometimes is even superior to them [16, 17]. Now the accuracy of the results is mainly determined by hardware and software resources used by researchers and their experience. Besides, the MC methods have some valuable advantages concerned with their rigid mathematical justification and the possibility of control over the accuracy of results by the resources of the methods themselves. Moreover, the results can be visualized and a great body of attendant information can easily be displayed. The weaknesses of these methods can be taken into account and their influence on the results of numerical calculations can easily be controlled [10, 12, 15].

MC methods have been successfully used to study a large number of systems undergoing phase transitions. The results of such investigations have been reviewed, e.g., in Refs [10, 16–18]. But so far the primary emphasis has been given to simple ferromagnetic systems with interacting nearest neighbors. The study of real substances with regard to their

concrete crystal structure, multispin and relativistic effects of interactions between next nearest and more distant neighbors has received less attention. Besides, in most works where the MC methods are used to investigate lattice models the critical region is treated only qualitatively. Therefore in this review we will deal mainly with the results obtained in the studies of systems near or at the critical point. Of all the extensive material on the subject we will consider only the papers where some original results are found, the CE and CA are calculated with high accuracy, and new methods and approaches are used to study PT and CP. Besides, we concentrate mainly on models treating magnetic PT and CP, since we believe that significant progress has been achieved there, and our review can bridge a gap concerned with the lack of analogous reviews in Russian literature.

This paper is arranged as follows. First we briefly describe the classical version of the MC method used in statistical physics (Metropolis algorithm), consider some most up-to-date highly efficient MC algorithms, discuss quantum MC methods, and outline the Handscomb approach. In Section 3 we discuss the results obtained in studies of phase transitions and static critical phenomena in model systems. Section 4 is devoted to the study of PT and CP in quantum-lattice systems. The results of investigations of real magnetic substances with the use of microscopic Hamiltonians are presented in Section 5. The data obtained in studies of critical dynamics by MC are considered in Section 6.

2. MC methods in statistical physics

2.1 Classical MC method

Let us consider a canonical ensemble consisting of N particles in a volume V at a temperature T . Since we will investigate models on a regular lattice, the variable V can be omitted, and therefore we will deal with two thermodynamic variables N and T . Below we will mainly use ‘magnetic’ jargon.

In statistical mechanics, the average of any smooth function $f(\mathbf{x})$ is written as [19]

$$\langle f(\mathbf{x}) \rangle = \frac{\int_V f(\mathbf{x}) P(\mathbf{x}) d\mathbf{x}}{\int_V P(\mathbf{x}) d\mathbf{x}}, \quad (2.1)$$

where $P(\mathbf{x})$ is the probability density for N dimensional vector \mathbf{x} in region V , $\mathbf{x} = (\mathbf{r}_1, \mathbf{r}_2, \dots, \mathbf{r}_N)$, where \mathbf{r}_i is the radius vector of the i th particle;

$$\int_V d\mathbf{x} = \int_V d\mathbf{r}_1 \dots \int_V d\mathbf{r}_N, \quad P_{eq}(\mathbf{x}) = P(\mathbf{x}) \sim \exp\left(-\frac{H_N(\mathbf{x})}{k_B T}\right). \quad (2.2)$$

Here $H_N(\mathbf{x})$ is the Hamiltonian of the system and k_B is the Boltzmann constant. Unfortunately, integrals of type (2.1), calculated by partition of the region V and random sampling of points, are of little interest in statistical physics. The MC method used in statistical physics is based on the idea of an ‘essential’ sample [10–12, 20, 21]. In this version the points are chosen in the region V so that their probabilities are proportional to their Boltzmann factor (2.2). Then expression (2.1) takes on the form

$$\langle f(\mathbf{x}) \rangle \approx \overline{f(\mathbf{x})} = \frac{\sum_{i=1}^N f(\mathbf{x}_i) P^{-1}(\mathbf{x}_i) \exp(-H(\mathbf{x}_i)/k_B T)}{\sum_{i=1}^N P^{-1}(\mathbf{x}_i) \exp(-H(\mathbf{x}_i)/k_B T)}. \quad (2.3)$$

Choosing $P(\mathbf{x}_i)$ in accordance with (2.2), expression (2.3) transforms into the mean average

$$\overline{f(\mathbf{x})} = \frac{1}{M} \sum_{i=1}^M f(\mathbf{x}_i). \quad (2.4)$$

In real systems the exact value of $P_{\text{eq}}(\mathbf{x}_i)$ is not known, but can be obtained by a random walk $\{\mathbf{x}_i\}$ in the phase space with the use of a Markovian process so that $\lim_{i \rightarrow \infty} P(\mathbf{x}_i) = P_{\text{eq}}(\mathbf{x}_i)$. The Markovian process is determined by the probability $W(\mathbf{x}_i \rightarrow \mathbf{x}_j)$ of the transition from a point \mathbf{x}_i to a point \mathbf{x}_j . The condition of microscopic reversibility provides a way to evaluate the probability $W(\mathbf{x}_i \rightarrow \mathbf{x}_j)$:

$$P_{\text{eq}}(\mathbf{x}_i)W(\mathbf{x}_i \rightarrow \mathbf{x}_j) = P_{\text{eq}}(\mathbf{x}_j)W(\mathbf{x}_j \rightarrow \mathbf{x}_i). \quad (2.5)$$

In accordance with (2.5), the ratio of transition probabilities depends only on the change in the energy $\Delta H = H_N(\mathbf{x}_j) - H_N(\mathbf{x}_i)$:

$$\frac{W(\mathbf{x}_i \rightarrow \mathbf{x}_j)}{W(\mathbf{x}_j \rightarrow \mathbf{x}_i)} = \exp\left(-\frac{\Delta H}{k_B T}\right). \quad (2.6)$$

Equation (2.6) does not determine unambiguously a single value of $W(\mathbf{x}_i \rightarrow \mathbf{x}_j)$, therefore the choice is carried out using the Metropolis algorithm [20–22]:

$$W(\mathbf{x}_i \rightarrow \mathbf{x}_j) = \begin{cases} \frac{1}{N} & \text{if } \Delta H \leq 0, \\ \frac{1}{N} \exp\left(-\frac{\Delta H}{k_B T}\right) & \text{if } \Delta H > 0, \\ 1 - \sum_{i \neq j} W(\mathbf{x}_i \rightarrow \mathbf{x}_j) & \text{if } i = j. \end{cases} \quad (2.7)$$

The above scheme based on the essential sampling provides a good accuracy for estimating $f(\mathbf{x})$ far away from the critical region with the use of rather few MC steps per particle (about $10^3 - 10^4$). Note that the error of estimating $\bar{f}(\mathbf{x})$ is expressed as

$$(\delta f(\mathbf{x}))^2 \approx \frac{1}{M(M-1)} \sum_{i=1}^M (\overline{f(\mathbf{x})} - f(\mathbf{x}_i))^2, \quad (2.8)$$

where $M \gg 1$, and M is the number of intermediate averages in K_0 steps. If the total number of steps is considered to be equal to K , then $M = K/K_0$.

Numerous investigations obtained by MC methods demonstrate that these methods are a powerful apparatus for studying classical systems [10–18, 20–22]. However, near the critical point the effectiveness of the method decreases sharply, and so-called critical retarding takes place. The critical retarding probably presents the gravest obstacle to the study of phase transitions and critical phenomena by MC methods.

According to the modern views of PT and CP, the relaxation time at the critical temperature T_c of phase transition is divergent [1, 2] as

$$\tau \sim \xi^z, \quad (2.9)$$

where ξ is the correlation length $\xi \sim (T/T_c - 1)^{-\nu}$ and z is the dynamic critical exponent. The typical value of the exponent z

is 2 for a large number of models [1, 2]. Thus, the relaxation time increases sharply as $T \rightarrow T_c$. The increase of τ to infinity makes the MC method inefficient near the point of the second-order transitions. The reason is that in the Metropolis algorithm, an MC test consists in flipping a single spin, while the phase phenomena near the critical points are caused by fluctuations of large-sized spin clusters.

In finite-sized systems used in numerical simulations, the cluster size is restricted by the size L of the system under consideration [18]. In this case, the relaxation time τ at $T = T_c$ is determined as

$$\tau \sim L^z. \quad (2.10)$$

Recently some new algorithms of the MC method have been proposed, which enable one to obviate the problem of critical retarding. Among these are multigrid algorithms [23–28], overrelaxation methods [29–32], algorithms based on the RG theory [33–36], and cluster algorithms [37–40], various versions of which based on the percolation approach [37, 38] are especially popular.

There are some other methods where various combined schemes are used to get around some particular problems [41–43]. For example, in Ref. [42] a Replica MC method was proposed to increase the efficiency of cluster algorithms as applied to the frustrated systems, while in Ref. [43] this method was used to study spin glasses, namely, Ising spin glasses in 2-, 3-, and 4-dimensional spaces [42, 44–46].

Among the new algorithms, the multicluster Swendsen–Jang method [37] and one-cluster Wolff approach [38] are the most efficient. We briefly outline them.

The *Swendsen–Jang algorithm* is based on two transformations:

- (1) a spin configuration is replaced by a configuration of spin bonds;
- (2) the configuration of bonds is used to produce a new spin configuration.

Both the operations deal with random numbers.

Bonds between the nearest neighbors S_j of a spin S_i arise with a probability $P = 1 - \exp(-K)$, where $K = J/k_B T$ if S_j has the same value as S_i . If the nearest spins S_i and S_j have different values, a bond between them does not form, and, as a result, they cannot be included in the same cluster. Within the limits of a single cluster, all the spins have the same value. Then the selected spin S_i is MC tested. On S_i taking a new value, the same value is applied to all the spins of the cluster. After that the procedure is repeated, starting with a new configuration.

The algorithm is most efficient for the vectorization of calculations and for large lattices. The high efficiency of the method is also supported by the values of z obtained in the Ising models. Thus, for a 2-dimensional system ($d = 2$), $z \approx 2.1$ if the conventional algorithm is used and $z \approx 0.35$ in the case of the Swendsen–Jang algorithm. In the three-dimensional model, the conventional method yields $z \approx 2$, while the Swendsen–Jang algorithm results in $z \approx 0.55$ [37]. This algorithm is easily extended to the case of antiferromagnetic interactions in an external magnetic field [37].

The *one-cluster Wolff algorithm* [38] differs from the Swendsen–Jang method in two points:

- (1) as in the above-described method, all the nearest neighbors of a chosen spin S_i are included in a cluster around this spin with the probability $P = 1 - \exp(-K)$. However, after that the second neighbors with the same spin are

included in the cluster, with the same probability and the procedure is repeated until the cluster reaches the boundaries of the system;

(2) the thus obtained cluster is reoriented with probability 1. Peculiarities of the application of this algorithm to models with continuous symmetry are considered in Ref. [38].

Note that for the three-dimensional Ising model this algorithm yields $z \approx 0.4$, arguing for its high efficiency with respect to the Swendsen – Jang method.

Both the algorithms are ergodic and nonlocal. Although they are widely used, the problem of which algorithm is more efficient, in particular, as applied to various models, is still unclear [39]. For example, according to Ref. [41], the Wolff algorithm is more efficient due to the fact that the average size of a cluster with changed spins is larger than that in the Swendsen – Jang method.

Note that some algorithms are not ergodic (for example, the Replica Monte Carlo method), while others correspond to the microscopic ensemble (overrelaxation method), and they should be combined with other methods, for instance, with the Metropolis algorithm [22].

2.2 Quantum Monte Carlo method

At present, the possibility of efficient application of the MC schemes in studies of quantum systems (in particular, lattice models with arbitrary spin in a wide range of varying physical parameters) is highly problematic. There are several approaches to the use of MC methods in such problems.

One of the approaches is based on the Trotter formula [47–52]

$$\exp\left(\sum_{i=1}^p A_i\right) = \lim_{n \rightarrow \infty} \left(\exp\left(\frac{A_1}{n}\right) \exp\left(\frac{A_2}{n}\right) \dots \exp\left(\frac{A_p}{n}\right) \right)^n, \quad (2.11)$$

which transforms any d -dimensional quantum system into a $(d+1)$ -dimensional classical system of a general type. This method was used to study the one-dimensional Ising [53], the one-dimensional Heisenberg, and the XY models [54, 55]. Most of the cited papers, especially [52], deal with the effects related to the finite value of the additional dimensionality (n). The additional dimensionality is usually considered as discrete imaginary time ($0 < n < \beta$, $\beta = 1/k_B T$). The use of formula (2.11) results in the division of the imaginary time scale into N discrete intervals of length Δn ($\beta = N\Delta n$); the division is valid when the additional dimensionality is infinite, but the latter cannot be realized in numerical calculations. This means that in the MC calculations with the use of the above procedure, one more error $\sim \Delta n^2$ arises in addition to the usual errors of the MC method that are related to the finite scale of the time interval. As the temperature decreases, the number N of time intervals should be magnified to keep the desired accuracy, leading to an increased time of calculations and multiplication of statistical errors. As a result, in the low-temperature region the calculations are rather difficult. Nevertheless, the approach was successfully used to study a large number of different models. Thus, Russian researchers have obtained some interesting results in studies of boson, fermion [56–62], and magnetic spin systems [63–65]. Recently the approach has been substantially modified. A highly efficient version of the MC method with the use of the Trotter expansion of the Gibbs exponent (2.11) was proposed in Ref. [66]. This so-called loop algorithm is rapidly convergent (the rate of convergence 100-fold exceeds the

conventional value) due to the use of a grand canonical ensemble and global changes in the state of the system in the course of MC modeling. However, this version also fails in the low-temperature region. An important step was taken in Refs [67, 68], where the authors proposed getting rid of the discrete Trotter expansion and using an expansion with continuous time $0 < n < \beta$ ($\Delta n \rightarrow 0$), which renders the method asymptotically correct. The idea was further developed in Ref. [69], where it was combined with the loop algorithm and applied to spin systems. However, these approaches are rather specific, cumbersome, and require additional modifications of algorithms in each case. All these difficulties seem to have been successfully obviated by N V Prokof'ev et al. [70, 71]. Their version of the MC method is characterized by rapid convergence, can treat various ensembles and global thermodynamic quantities at any temperature. Evidently, to reveal all the advantages and drawbacks of this extremely interesting method, one should apply it to a large number of different models.

Quantum MC methods include one more approach, which treats the partition function as the sum of all possible products of interacting parts of the system under consideration. Clearly, the problem of imaginary time does not arise here. The products form a set on which a Markov chain is determined. This approach was first proposed by Handscomb in Ref. [72] and used to calculate thermodynamic properties of the isotropic Heisenberg model with spin $S = 1/2$ [73]. The approach was somewhat improved in Refs [74, 75], where some critical exponents were calculated for the one-dimensional Heisenberg model with $S = 1/2$. A similar model was also studied in Refs [76–78], while the XY model was investigated in Ref. [79]. Some interesting data were obtained by I A Favorskii and P N Vorontsov-Vel'yaminov et al. [80–87]. The Handscomb method was extended in Refs [81, 82] to the Ising model with a transverse field and short- and long-range interactions. Ingenious results of the study of the quantum Heisenberg model with multispin exchange on a simple cubic lattice with $S = 1/2$ were obtained in Refs [81, 83, 84]. The generalization of the method to the Heisenberg model with multispin exchange was carried out in Ref. [84]. Note that the papers [81, 83] were the first to study first-order phase transitions by the quantum MC method.

Here we outline the Handscomb method following [82, 85]. Let the Hamiltonian of a system take on the form of the operator sum

$$H = -2\mu H^* \sum_{i=1}^N S_i - 2J \sum_{i=1}^{N_b} S_{i(i)} S_{i'(i)} = H_0 + \sum_{i=1}^{N_b} H(i), \quad [H(i), H_0] = 0, \quad (2.12)$$

where N is the number of spins, N_b is the number of bonds, and H^* is the magnetic field. If we write the canonical average of an operator A as

$$\langle A \rangle = \frac{\text{Sp}\{A \exp(-\beta H)\}}{\text{Sp}\{\exp(-\beta H)\}}, \quad (2.13)$$

then the numerator of (2.13) is expressed as

$$\text{Sp}\{A \exp(-\beta H)\} = \sum_{r=0}^{\infty} \sum_{c_r} \left[\frac{(-\beta)^r}{r!} \right] \text{Sp}\{A H(i_1) H(i_2) \dots H(i_r) \exp(-\beta H_0)\}, \quad (2.14)$$

where C_r is the set of exponents i_1, i_2, \dots, i_r , characterizing bonds; and \sum_{C_r} is the sum over all the r elementary sets C_r . If we change the order of calculating the trace and the sum, the partition function can be presented as

$$Z = \text{Sp}\{\exp(-\beta H)\} = \text{Sp}\left\{\exp(-\beta H_0) \sum_{r=0}^{\infty} \left[\frac{(-\beta)^r}{r!}\right] \times \sum_{C_r} (H(i_1)H(i_2)\dots H(i_r))\right\}. \quad (2.15)$$

Then the average of any observed quantity A is determined as the value of the mathematical expectation Ω_A defined in the space of all possible sequences C_r as:

$$\Omega_A(C_r) = \frac{\text{Sp}\{AH(i_1)H(i_2)\dots H(i_r)\exp(-\beta H_0)\}}{\text{Sp}\{H(i_1)H(i_2)\dots H(i_r)\exp(-\beta H_0)\}}. \quad (2.16)$$

To construct a Markov chain, we can use the relation between the spin operators $S_i, S_{i'}$ ($S = 1/2$) and the permutation operators $E(t, t')$:

$$E(t, t') = \frac{1}{2}(4S_i S_{i'} + 1). \quad (2.17)$$

The operator $E(t, t')$ changes the spin numbered t to the spin numbered t' and vice versa. We use the notation

$$\pi(C_r) = \left[\frac{(-\beta)^r}{r!}\right] \text{Sp}\{H(i_1)H(i_2)\dots H(i_r)\exp(-\beta H_0)\}. \quad (2.18)$$

In the case of a ferromagnet, we have $H(i) = -JE(t_i, t'_i)$, whence

$$\begin{aligned} \pi(C_r) &= \left[\frac{(-\beta J)^r}{r!}\right] \left\{ \prod_{i_k=1}^r E(t(i_k), t'(i_k)) \exp(-\beta H_0) \right\} \\ &= \left[\frac{(-\beta J)^r}{r!}\right] \prod_{j=1}^{K(C_r)} 2 \cosh\left(\frac{\mu \beta H a_j}{2k_B T}\right), \quad \pi(C_r) \geq 0, \end{aligned} \quad (2.19)$$

where $K(C_r)$ is the number of cyclic permutations to which the sequence C_r can be reduced, while a_j is the length of the j th cycle. As a result, we can write the partition function as the sum over $\pi(C_r)$

$$Z = \sum_{r=0}^{\infty} \sum_{C_r} \pi(C_r), \quad (2.20)$$

and construct the Markov chain in the space of exponent sets $\{C_r\}$ distributed with the normalized probability $P(C_r)$

$$P(C_r) = \frac{\pi(C_r)}{Z} \geq 0, \quad \sum_{C_r} P(C_r) = 1. \quad (2.21)$$

Finally, the average is determined as

$$\langle A \rangle = \sum_{r=0}^{\infty} \sum_{C_r} \Omega_A(C_r) P(C_r) = \varepsilon\{\Omega_A(C_r)\}. \quad (2.22)$$

The rules for constructing a stochastic procedure and specific details are given in Refs [82, 84, 85]. At present, serious efforts are still being made to develop quantum MC methods suitable to study systems with an arbitrary spin [67, 70, 71, 88–90].

3. Studies of PT and CP in model systems

Essentially all the studies of various models of phase transitions by MC methods have been accompanied by attempts to investigate the critical region and calculate CE and CA [15, 16, 91–93]. However, in earlier works almost without exception this region was considered only qualitatively. It was rather difficult to calculate T_c and other critical parameters with a high accuracy. The situation seems to have changed when K Binder proposed to use the fourth-order cumulants U_L to determine T_c [94, 95]

$$U_L = 1 - \frac{\langle E^4 \rangle_L}{3\langle E^2 \rangle_L^2}, \quad (3.1)$$

$$U_L = 1 - \frac{\langle M^4 \rangle_L}{3\langle M^2 \rangle_L^2}, \quad (3.2)$$

where E is the energy of the system with a characteristic linear size L , and M is the magnetization.

Expressions (3.1) and (3.2) allow one to calculate T_c with a high accuracy in the systems undergoing first- and the second-order phase transitions, respectively. In the first-order phase transitions, the value U_L tends to a nontrivial limit. In the case of the second-order phase transitions, the temperature dependence of U_L can be obtained at various L and T_c as the point of intersection of the curves. The theory of finite-size scaling implies such a point to exist [12, 16, 96] (the theory is also detailed in Section 5). Figures 3 and 4 plot typical temperature dependences of U_L (in Fig. 4 and below, the error of all the plotted quantities corresponds to the scale of the used symbols). The accuracy of the method of cumulants is rather high, although it requires considerable computing resources and careful treatment of the results. The method can be applied to various problems such as the Ising and Heisenberg models [94–98], the Potts [99] and the XY [100] models, including spin glasses [101], and others.

The next great stride forward in this direction was the design of highly efficient cluster algorithms for the MC methods, which were specially devised to study the critical region and treat histogram data [37–40]. All these developments in combination with the theory of finite-size scaling

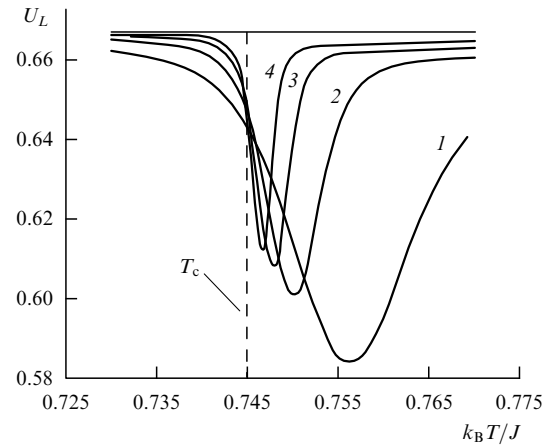


Figure 3. Temperature dependence of the Binder cumulant U_L for the first-order phase transition in the 2d Potts model with $q = 8$ states: 1, $L = 16$; 2, 24; 3, 32; and 4, 40 [130].

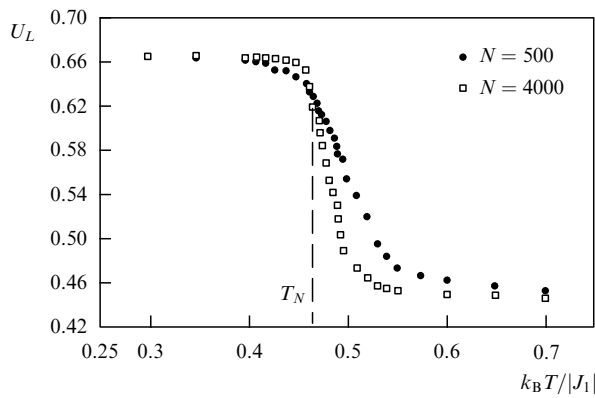


Figure 4. Temperature dependence of the Binder cumulant U_L for the second-order phase transition in the ferromagnetic Cr_2O_3 model.

have enabled one to obtain results by the MC method, whose accuracy is highly competitive with that found by other methods (see Figs 1 and 2).

A detailed study of the Ising model on squared and simple cubic (SC) lattices was carried out as early as in the 1970s [92, 93]. In succeeding years the emphasis has been displaced toward the study of more realistic models with complex interactions on other types of lattices including rather exotic ones. For example, the Ising model with three-spin and four-spin interactions was studied in Ref. [102] and [103], respectively. In Refs [104–107] it was applied to random fields. In Ref. [108] a biquadratic interaction was considered. In Ref. [109] the model was investigated in a transverse field and in Ref. [110] it was studied in a strong magnetic field. Besides, it was applied to dilute [111] and anisotropic [112] systems as well as to antiferromagnetic [113, 114] and frustrated systems, with account of the interaction of next-nearest and more distant neighbors [116–118] and to quasilattices [119, 120].

The equilibrium properties of the Heisenberg model and its various versions were studied in Refs [121–129]. The Potts model was considered in Refs [130–133]. The MC method is intensively applied to XY, XXZ, and XYZ models on lattices of various space dimensions [134–141].

In recent years the MC method has probably been playing a key role in determining whether or not a model belongs to a certain universality class and in checking the validity of the universality hypothesis for various models.

Let us consider some results obtained in various models, which seem to be the most interesting.

The 2d ferromagnetic Ising model was studied on a quasiperiodic octagonal lattice with free boundaries ($L \times L = N$, $185 \leq N \leq 5497$). The critical value T_c found by the MC method is considerably higher ($k_B T_c / J = 2.39 \pm 0.01$) than that found in the classical Ising model on a square lattice ($k_B T_c / J = 2.269$), although the coordination number is the same for both the models and equal to $n = 4$. The critical exponents ν , β , and γ agree with data obtained on a quasilattice with a 5-fold symmetry axis (Penrose lattice). Careful investigations on this lattice demonstrated that the finite-size scaling well describes quasilattices with free boundaries, which suggests that the quasilattice 2d Ising model without frustrations belongs to the same universality class as the 2d Ising model with periodic boundary conditions (PBC). Besides, the authors of [119] easily calculated γ and ν ,

but met with serious difficulties in determining β because of its small value. Noteworthy also is the fact that the critical temperature T_c for the octagonal and the Penrose lattices is higher than that for an infinite square lattice. But the present numerical calculations do not allow one to determine whether or not the critical temperatures T_c are the same for both types of quasilattice.

The Ising model was studied in Ref. [120] on a 2d random lattice with the number of spins equal to $N = 5000, 10000, 20000, 40000, 80000$. The main goal of the work was to test the validity of the universality hypothesis for random lattices. Earlier attempts to do this have not been successful [142–145]. Note that the conventional MC algorithm used in some works [145] requires too much time for numerical calculations; therefore, since the late 1980s, cluster algorithms have come into wide use. Such an algorithm was used for an MC study in Ref. [120]. The most probable coordination number $n = 6$ for the lattice concerned is the same as for a regular triangular lattice. The value $K_c = J/k_B T_c = 0.2630 \pm 0.0002$ obtained in [120] by the calculations of the Binder cumulant agrees well with that found by high-temperature expansion (HTE) [145], and is close to that for the regular triangular lattice $K_c = \ln(3/4) = 0.27465$. The values obtained for the critical exponents ν , β/ν , γ/ν , and γ bring out clearly that the 2d Ising model on a random lattice belongs to the same universality class as the Ising model on a regular 2d lattice.

Extensive studies of the Ising model as applied to random fields on an SC lattice of $L \times L \times L$ size ($4 \leq L \leq 32$) were carried out in Ref. [107]. Using finite-size scaling and a cluster algorithm, the authors calculated by the MC method ν , β , γ and critical temperatures as functions of a random field h . The CEs were compared with data obtained by other methods (the conventional MC approach, HTE and RG theory) and the results found by the cluster MC algorithm were shown to be more accurate.

Noteworthy is an interesting feature obtained in Ref. [137] for the completely frustrated XY model on a 2d square lattice by the MC method. There the critical exponents were found to be $\nu = 0.3069$, $\eta = 0.1915$; for lattices of sizes up to $L \times L = 240 \times 240$, the model was revealed to belong to a universality class different from that of the conventional XY model and the classical 2d Ising model. At the same time the authors point out that the results should be carefully checked.

The most exact values of critical parameters of the three-dimensional Ising model on an SC lattice seem to have been obtained in Ref. [146] by the classical MC method. The critical properties of the Ising model on lattices of size $8 \leq L \leq 96$ were considered using histogram analysis and special multispin algorithms. Table 1 presents the comparison

Table 1. Critical parameters for the 3d Ising model.

Critical parameter	Field theory		MC method Metropolis algorithm [146]
	[6, 7]	[8]	
K_c	—	—	0.2216595(26)
ν	0.6305(25)	0.631	0.6289(8)
α	0.108(9)	0.107	0.113*
β	0.3265(25)	0.327	0.3258(44)
γ	1.239(4)	1.239	1.2390(71)
η	0.037(3)	0.038	—
δ	4.795(17)	4.7889*	4.8029*

* The values are calculated with the use of the relations $\alpha + d\nu = 2$ and $\delta = 1 + \gamma/\beta$.

of the obtained results with the widely used [6, 7] and new [8] data calculated on the basis of the field theory.

There are a number of works where the Heisenberg model is treated with a high accuracy [128]:

$$H = -J \sum_{i \sim j} (S_i^x S_j^x + S_i^y S_j^y + S_i^z S_j^z), \quad (3.3)$$

where $J > 0$ is the parameter of the exchange interaction $|\mathbf{S}_i| = 1$. The studies cited were carried out on an SC lattice of size $L \times L \times L$ ($6 \leq L \leq 24$). In Refs [39, 40] the equilibrium critical exponents α , β , γ , and ν were calculated with a high degree of precision using finite-size scaling and optimized histogram analysis. In Ref. [147], model (3.3) was studied on SC and BCC lattices of sizes up to $L = 40$. The authors calculated various thermodynamic quantities as a function of temperature near T_c and showed that although the critical temperatures for these lattices [$K_c = 0.693035(37)$ for the SC lattice and $K_c = 0.486798(12)$ for the BCC lattice] differ significantly, the critical exponents correlate well for both the lattices. Similar investigations were performed in Ref. [148], where the sought effect was checked by the cluster algorithm on an SC lattice of size $L \leq 48$. The data were thoroughly analyzed by the histogram method, and ν , α , β , γ , and η were calculated with the use of finite-size scaling. The results obtained in all the cited works are listed in Table 2. As is seen, they are in excellent agreement with the data found by the RG method and the ε expansion. The authors of Ref. [148] also studied spatial correlations and susceptibility for the high-temperature phase on lattices of sizes up to $L = 100$. Their results suggest that ν and γ can be evaluated directly from the MC data on power dependences without invoking any other methods. If this is the case, then bearing in mind the pace of the development of computing resources, one would expect that in the short run critical parameters may be calculated directly from the MC experiments without resorting to any contrivances or technical expedients. In Section 5 we will demonstrate that some critical exponents of ferromagnetic models can be evaluated in this way for systems of far smaller size.

Of great interest are the results of the MC study of frustrated models. On the whole, the question of the

existence of a new chiral class of universality for frustrated spin systems on various lattices, in particular, on triangular ones, is a subject of controversy today [149]. In Refs [150, 151] the critical behavior of the frustrated antiferromagnetic XY model and Heisenberg model on a hexagonal lattice was assumed to be described by the universality class characterized by the exponents

$$\alpha = 0.24(8), \quad \beta = 0.30(2), \quad \gamma = 1.17(7), \quad \nu = 0.59(2), \\ \beta_{\text{ch}} = 0.55(4), \quad \gamma_{\text{ch}} = 0.72(8), \quad \nu_{\text{ch}} = 0.60(3)$$

(for the $n = 3$ Heisenberg model), where ch denotes chirality. In this respect noteworthy are the data obtained in Ref. [149] for the frustrated Heisenberg model on a hexagonal lattice of sizes $12 \leq L \leq 36$. The authors found that the temperatures of magnetic and chiral ordering coincide within the calculated accuracy $T_c = T_{\text{ch}} = 0.9577(2)$, but the reasons of this coincidence remained unclear. They revealed a continuous character of phase transition in this model, having calculated the Binder cumulant. Besides, they found the critical exponents β , γ , ν , β_{ch} , γ_{ch} , and ν_{ch} , and showed that although $T_c = T_{\text{ch}}$, the exponents ν and ν_{ch} are not equal, which suggests different characters of the growth of magnetic and chiral correlations. The values of CE obtained there count in favor of the hypothesis of the existence of a new universality class. At the same time, the authors believe that more detailed studies are necessary for the issue to be resolved conclusively.

Noteworthy is another interesting work [152], where a liquid with the Heisenberg spins and Heisenberg interaction was studied. In this liquid, an order–disorder phase transition occurs as temperature changes while the spin density is fixed. Using finite-size scaling theory, the authors calculated the temperature of phase transitions and CE at various spin concentrations. They revealed that the exponents β/ν , γ/ν , and $1/\nu$ are the same for all the densities studied ($p = 0.4, 0.6, 0.7$) and differ from those for the lattice Heisenberg model.

4. Phase transitions and critical phenomena in quantum lattice models

In this section we consider rigorous results obtained by the quantum MC method within the Handscomb approach. After the method was used to study the ferromagnetic Heisenberg model in the early sixties [72, 73], it was not called for over a long period of time until it was applied in Refs [74, 75]. Paper [74] dealt with one-dimensional ferromagnetic and antiferromagnetic systems and the three-dimensional ferromagnetic Heisenberg model with $S = 1/2$. The values of the susceptibility, heat capacity and energy calculated there agree well with the data obtained by HTE. In Ref. [75] some critical exponents for the classical Heisenberg chain were calculated (for example, $\gamma = 1.75$) and, what is more important, the method was shown to suit to the low-temperature region down to $k_B T/J = 0.025$, where the approach based on the use of the Trotter formula is impractical. However, it is not only this fact that provoked interest in the studies under discussion. The low-temperature behavior of the one-dimensional ferromagnetic Heisenberg chain raised a heated debate [153] during which many points were clarified due to the quantum MC method. As $T \rightarrow 0$, the susceptibility exponent γ behaves as $\chi \sim \varepsilon^{-\gamma}$, various methods yield a wide scatter in the data ($\gamma \sim 1.3 - 2.0$), and the most reliable result ($\gamma = 2.0$) was probably found proceeding from the Bethe ansatz [154]. But this approach involves a

Table 2. Critical parameters for the 3d Heisenberg model.

Critical parameter	Field theory		MC method	
	[6, 7]	[8]	Metropolis algorithm [128]	Cluster algorithm
K_c	—	—	0.6299(1)	0.693035(37) [147] 0.6930(1) [148]
ν	0.710(7)	0.706	0.706(9)	0.7048(30) [147] 0.704(6) [148]
α	−0.130(21) −0.115(9)	−0.117	−0.118(27)	−0.1144(90) [147] −0.112(18) [148]
β	0.368(4)	0.366	0.364(7)	0.3639(35) [147] 0.362(4) [148]
γ	1.390(10)	1.386	1.390(23)	1.3873(89) [147] 1.389(14) [148]
η	0.033(4)	0.038	0.031(7)	0.027(2) [148]
δ	4.777(14)	4.8187*	4.819	—

* The values are calculated from the relations $\alpha + d\nu = 2$ and $\delta = 1 + \gamma/b$.

complicated calculation procedure, i.e., a large set of non-linear integral equations should be solved with a high accuracy and then double extrapolation of the data should be performed ($N \rightarrow \infty$, and the anisotropy parameter $D \rightarrow 1$). Actually, the value of this exponent in Ref. [154] did not exceed 1.9. Having extrapolated it to $T = 0$, the authors arrived at $\gamma = 2$. Earlier studies by the quantum MC method also resulted in discrepant results ($\gamma \approx 1.3$, $\gamma \approx 1.55$ [153], $\gamma \approx 1.75$ [75]), which was probably caused by the insufficient number of spins and insufficiently low temperatures considered there ($N \leq 200$, $T \geq 0.025$). For example, in Ref. [75] $N = 128$ and $T = 0.025$ were used. To clarify the question, the authors of Ref. [81] dealt with larger MC cells and the number of spins equal to $N = 100, 200, 300, 500$ at still decreased temperatures ($0.01 \leq k_B T/J \leq 0.1$). At each temperature, saturation with respect to N was attained, i.e., a further increase in temperature did not affect the susceptibility, and the length of Markovian chains was about 5000 MC steps per spin. The susceptibility exponent γ_{ef} was determined by differentiating the dependence of $\ln \chi$ on T . The extrapolation of the MC data to $T \rightarrow 0$ yields $\gamma \approx 2.0$, which agrees well with the data obtained using the Bethe ansatz [154].

In Refs [80, 82] the method was extended to the Ising model subjected to a transverse field with arbitrary long-range potentials J/N . The results obtained were compared with those found by the molecular field theory and by the conventional MC method. Besides, in Ref. [80] the method in question was first applied to study the Heisenberg model ($d = 1$, $S = 1/2$, $N = 51$) with long-range potentials $J \sim r^{-3}$. Low-temperature data were used to estimate the susceptibility (at $T \rightarrow 0$), which was found to be $\gamma = 1.70 \pm 0.05$. This value agrees with the result obtained in Ref. [75] within the accuracy of the method.

The quantum MC method based on the Handscomb approach proved to be useful in studies of both first- and second-order phase transitions. It can also treat Hamiltonians with multispin interactions. Such investigations were carried out in [83], where the quantum Heisenberg model ($S = 1/2$) was studied on an SC lattice with the Hamiltonian

$$\hat{H} = - \sum_{s>p} 2J_{sp}(\hat{S}_s \hat{S}_p) - \sum_{k,l,m,n} 2K_{klmn}(\hat{S}_k \hat{S}_l)(\hat{S}_m \hat{S}_n), \quad (4.1)$$

where $J_{sp} = J > 0$ and the first sum includes only the nearest neighbors, while in the second term the exchange constants K_{klmn} are not zero ($K_{klmn} = K > 0$) only when the nodes k, l, m , and n form a unit square on the lattice.

The interest in the systems under discussion has several causes: multispin interactions take into account lattice vibrations in the first approximation and, besides, there are a number of real magnets where multispin interactions play a key role [155, 156].

The models described by a Hamiltonian of the type of (4.1) were considered earlier by the theory of molecular field (MF) [155] and by the method of Green's functions [154]. Both methods are approximate for Hamiltonian (4.1); for example, the molecular field method predicts that the second-order phase transition temperature T_c is independent of $\Delta = K/J$, while various schemes to uncouple the relations in the method of Green's functions result in a noncontrolled error [155].

In Ref. [84] the quantum MC method was extended to the considering the multispin interactions in the Hamiltonian. In [83], the systems (4.1) were studied by the extended method on

an SC lattice with periodic boundaries, containing $N = L \times L \times L$ spins ($L = 8, 12, 16$). The calculations were carried out for $\Delta = K/J = 0, 0.5, 0.75, 1.0$. The extension was performed without any approximations; therefore, the accuracy of the method at $\Delta > 0$ can be estimated in the limit $\Delta = 0$ for which there are rigorous data obtained by the HTE method with consideration of the terms up to the tenth order [157]. At $\Delta = 0$, a second-order phase transition takes place. The data on the temperature dependence of the energy presented in Ref. [83] agree well with those obtained by HTE. The critical temperatures calculated by the MC and HTE methods also coincide within the accuracy of the method [157]:

$$T_c^{\text{MC}} = \frac{k_B T}{J} = 1.67 \pm 0.03, \quad T_c^{\text{HTE}} = 1.68 \pm 0.01,$$

while the molecular field approach and the method of the Green's functions result in

$$T_c^{\text{MF}} = 3.0, \quad T_c^{\text{GF}} = 2.4 \pm 0.2.$$

According to both the methods (MF and GF), at $\Delta > \Delta_0$ the second-order phase transitions change to the first-order ones ($\Delta_0^{\text{MF}} = 0.33$, $\Delta_0^{\text{GF}} = 0.5$ [154]). Since the first-order phase transitions studied in Ref. [154] by the quantum MC method were not investigated before, we consider them in greater detail. At $\Delta = 0$ and 0.5 , the temperature dependence of the energy is smooth. However, at $\Delta = 1.0$ the dependence becomes discontinuous, although the gap is not large, which points to the first-order phase transition close to the second-order one. With this type of phase transition, finite-size systems exhibit sharp 'jumps' between phases, and the data are averaged (Fig. 5). The distribution along the Markovian chain indicates the presence of two branches in the tempera-

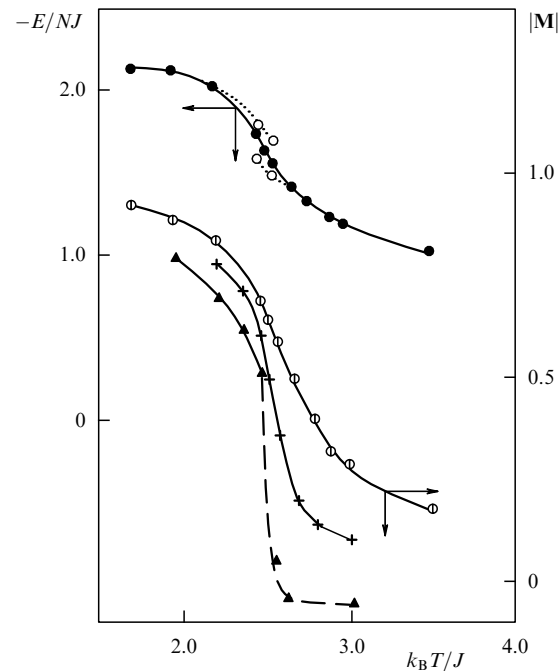


Figure 5. Temperature dependences of energy and magnetization at $\Delta = K/J = 1$. For the energy ($N = 512$), the symbols \bullet correspond to averaging over the whole Markovian chain, while symbols \circ refer to the data derived from the positions of maxima of the bimodal energy distribution. For magnetization, the symbols \circ correspond to $N = 512$; $+$, to $N = 4096$; and \blacktriangle , to $N = \infty$ [83].

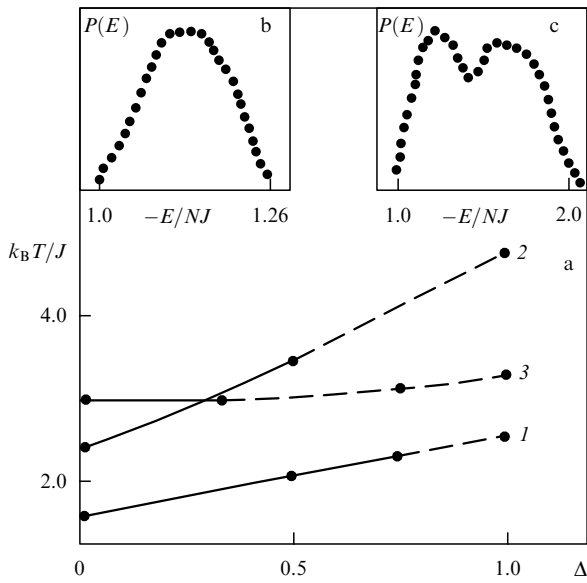


Figure 6. (a) Phase diagrams: 1, obtained by the MC method, 2, by Green's function method, 3, in the MF approach. Solid lines correspond to the second-order phase transitions, while the dashed ones, to the first-order phase transitions. (b, c) Energy distribution (in arbitrary units): (b) $\Delta = 0$, and (c) $\Delta = 1$ [83].

ture dependence of the energy; at $\Delta = 1$, the distribution is bimodal (Fig. 6c), while at $\Delta = 0, 0.5$ (second-order phase transition), it is Gaussian (Fig. 6b).

Figure 5 plots the magnetization of finite-size systems containing $N = 512$ and $N = 4096$ spins and their extrapolation to $N = \infty$. As is seen, there is a discontinuity at $N = \infty$. According to estimates [83], the value $\Delta_0 \approx 0.75$ is the limiting point separating first- and second-order phase transitions. Figure 6a depicts the phase diagrams of the model and their comparison with the data obtained in the MF approach and by the method of Green's functions. It is evident that the latter differ significantly from the MC results; both theoretical methods yield substantial errors. These results seem to suggest that the developed quantum MC method is highly efficient and can treat multispin exchange for the isotropic Heisenberg model.

The quantum MC method based on the Trotter transformation (2.11) turned out to be efficient to study magnetic systems with multispin interactions [47–52, 158]. Thus, S. S. Aplesnin [63, 64] investigated the thermal and magnetic properties and calculated two- and four-spin correlation functions for a one-dimensional antiferromagnetic chain with four-spin interactions and $S = 1/2$. It was shown that this interaction produces dimers in the chain and the dimer-paramagnetic phase transition is of the second order. An anisotropic antiferromagnet with four-spin interactions and $S = 1/2$ was also studied by the same method on a square lattice. The classical Heisenberg model with anisotropic bilinear and four-spin exchange was investigated in Ref. [159] by the conventional MC method.

5. Studies of PT and CE in models of real magnetic substances

5.1 CE in small magnetic particles

As already noted, most recent numerical studies of PT and CE have been centered on the well known ferromagnetic models

with interactions between nearest neighbors. For the most part, these models are the simplest ones and ignore many features of real systems.

In this section we consider the results obtained by the MC study of real magnetic samples. Such models take into account the peculiarities of real crystals, which are not considered in the simplest models but affect the critical behavior and the properties near T_c .

Models of the real ferromagnetic oxides α - Fe_2O_3 , Cr_2O_3 , and V_2O_3 were developed in Refs [129, 160–163], where their equilibrium magnetic and thermal properties were studied by the MC method, and short-time dynamic characteristics were analyzed by the MD method. These works deal with the main features and processes related to the influence of temperature, external magnetic field, shape of particles, the number of interacting elements and others effects on the properties of small magnetic particles and systems with periodic boundary conditions ($N_{\text{ef}} \rightarrow \infty$).

The critical behavior of complicated real systems has not been investigated in detail so far. Here, we dwell upon the results of our study of the critical behavior of model antiferromagnetic Cr_2O_3 . We consider the critical behavior of both small magnetic particles Cr_2O_3 and systems with periodic boundary conditions.

In recent years the properties of small particles have attracted ever growing attention. On the one hand, their practical application offers much promise [164–173]. On the other hand, small particles (clusters) are mesoscopic objects, i.e., they can be considered as a bridge between the classical microworld and quantum microworld [174–180]. Despite a large number of works devoted to small particles, their critical properties are still to be understood.

All crystallographic, exchange, and other parameters of the models of small particles considered in this review are taken from the experimental data and correspond to real Cr_2O_3 samples.

The Hamiltonian of the system can be written as [160]

$$H = -\frac{1}{2} \sum_{i,j} J_1(\mathbf{\mu}_i \mathbf{\mu}_j) - \frac{1}{2} \sum_{k,l} J_2(\mathbf{\mu}_k \mathbf{\mu}_l) - D_0 \sum_i (\mathbf{\mu}_i^z)^2, \quad |\mathbf{\mu}_i| = 1. \quad (5.1)$$

According to the data on neutron scattering and the theory of spin waves presented in Ref. [181], J_1 is the parameter of interaction of a spin with a nearest neighboring spin separated from it by a distance $r_{ij} = 2.65 \text{ \AA}$, while J_2 is the parameter of its interaction with the next three neighboring spins separated from this spin by a distance $r_{ij} = 2.89 \text{ \AA}$ ($J_2 = 0.45J_1$, $J_1 < 0$, $J_2 < 0$). The parameters of interactions of more distant spins were considerably less and not taken into account. The axis Z coincided with the direction of the diagonal of the rhombohedral unit cell [111]. Various relativistic interactions are approximated by an effective anisotropy $D_0 > 0$ [182, 183]. The ratio between the anisotropy and exchange was taken to be $D_0/|J_1| = 0.025$.

The calculations were carried out for spherical particles with diameters

$$d = 24.0, 28.4, 32.8, 34.8, 41.82, 46.4, 48.64 \text{ \AA},$$

the number of spins in the particles was respectively equal to

$$N = 286, 508, 760, 908, 1602, 2170, 2502.$$

Markovian chains of length up to 10×10^4 MC steps per spin were generated in the process. To equilibrate the system, a nonequilibrium portion of the chain of length $(5-20) \times 10^3$ MC steps per spin, depending on the proximity to the critical region, was ignored. Traditionally, when studying critical phenomena by the MC method, researchers try to decrease the influence of the free surface and impose various periodic boundary conditions on the system under study [10]. Here, we consider both systems with free surfaces and those with periodic boundary conditions. The questions related to magnetic properties [165, 172, 173] and critical phenomena in small particles [165], as well as the dependence of CE and CA on the presence of surface spins occurring under slightly different conditions than those of the bulk phase are of interest by themselves [184]. In the case under consideration, the fraction of surface spins varied over the range from 46.8% for the smallest particle to 22.8% for the particle containing $N = 2502$ spins. Since the total number of surface spins in particles is rather large, their influence on various thermodynamic parameters can be essential. To reveal the temperature dependences of heat capacity and susceptibility, we used the following expressions [128]:

$$C = (NK^2)(\langle U^2 \rangle - \langle U \rangle^2), \quad (5.2)$$

$$\chi = (NK)(\langle m^2 \rangle - \langle m \rangle^2), \quad (5.3)$$

where $K = |J_1|/k_B T$, N is the number of particles, U is the internal energy, and m is the sublattice magnetization.

The temperature dependences C and χ have clearly defined maxima in the critical region. It is known that for small particles the T_N value shifts to lower temperatures than in the case of systems containing substantial number of particles. In our experiments, we observed a pronounced shift of the maxima of C and χ as N changed (Figs 7a and 8a) [185–187], which suggests that the phase transition

temperature increases as the number of spins in the particles rises.

To approximate the critical behavior of heat capacity, we used the expressions [188–191]

$$C = \frac{A}{\alpha} |\varepsilon|^{-\alpha} (1 + D_c |\varepsilon|^x), \quad (5.4)$$

$$C = \frac{A}{\alpha} (|\varepsilon|^{-\alpha} - 1) + D_c |\varepsilon|^x, \quad (5.5)$$

where $\varepsilon = |T - T_c|/T_c$; A is the critical amplitude; D_c is the scaling correlation amplitude; and $x = 0.55$, corresponding to the Heisenberg model [6, 7].

The MC data were treated by the nonlinear least-squares method. The values α , A , and D_c minimizing the sum of mean deviations were considered to be optimal. The data calculated by (5.4) and (5.5) are in good agreement, but we preferred (5.5), since it provided higher accuracy.

The data obtained for α and A are listed in Table 3 [185]. All α values are negative at $T > T_N$, which is typical of the critical behavior of the Heisenberg model, but they are somewhat smaller than the theoretical value $\alpha = -0.126(28)$ obtained for the isotropic Heisenberg model with short-range

Table 3. Effective values of the critical exponent α and critical amplitudes A and A' for small particles ($\alpha' = \alpha$).

N	$5 \times 10^{-3} \leq \varepsilon \leq 7.5 \times 10^{-1}$			$2.5 \times 10^{-2} \leq \varepsilon \leq 7.5 \times 10^{-1}$		
	α	A	A'	α'	A	A'
286	-0.20(3)	0.61	0.61	-0.19(3)	0.60	0.59
508	-0.18	0.57	0.55	-0.17	0.56	0.56
760	-0.20	0.67	0.67	-0.20	0.65	0.66
908	-0.17	0.57	0.58	-0.16	0.55	0.57
1602	-0.19	0.66	0.60	-0.19	0.64	0.59
2170	-0.17	0.61	0.64	-0.17	0.60	0.63
2502	-0.21	0.63	0.68	-0.20	0.62	0.67

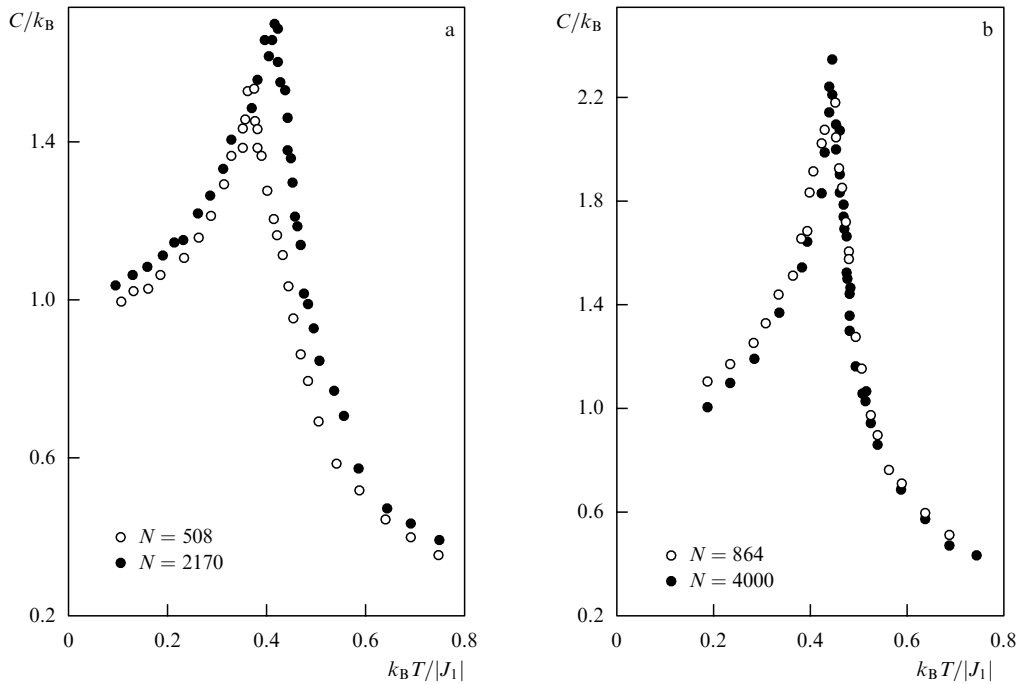


Figure 7. Dependence of the heat capacity C/k_B on the temperature $k_B T/|J_1|$ in the antiferromagnetic Cr_2O_3 model: (a) small particles [185], and (b) systems with periodic boundary conditions (model I).

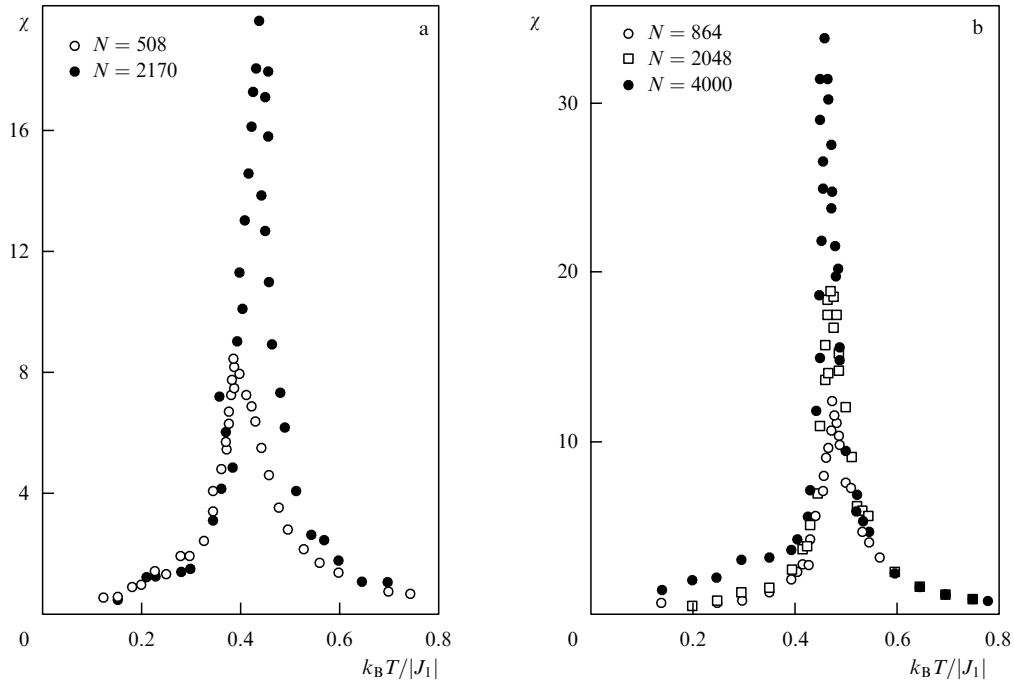


Figure 8. Dependence of the susceptibility χ on the temperature $k_B T/|J_1|$ in the antiferromagnetic Cr_2O_3 model: (a) small particles [185], and (b) systems with periodic boundary conditions (model I).

forces [6–8] and virtually do not depend on the sizes of particles. The values of A' at $T < T_N$ were obtained on the assumption that $\alpha' = \alpha$, in accordance with the equilibrium scaling theory [1, 2]. The relations between the critical amplitudes A and A' determined in the above-described way for all the particles lie in the range $0.95 \leq A/A' \leq 1.10$. The values of the critical exponent α for Cr_2O_3 derived from the experimental data are contradictory and vary from $\alpha = 0.14$ to $\alpha = -0.12$ [189, 190], depending on the method used, the interval of changes in ε , the choice of T_N and some other parameters.

Note that since Hamiltonian (5.1) includes a term describing anisotropy of single ions, a crossover from the Heisenberg type of the critical behavior of Cr_2O_3 to the Ising type should be observed [2, 191]. For all the calculated data, the crossover temperature $\varepsilon = (D_0/J)^{1/f}$ is about $\varepsilon_{\text{cr}} \approx 0.052$, where $f = 1.25$ at crossover from $n = 3$ to $n = 1$ (n is the number of components of the order parameter). But the values of α obtained in the temperature range $5 \times 10^{-3} \leq \varepsilon \leq 7.5 \times 10^{-1}$ do not suggest the occurrence of a crossover. The reason is probably that the surface spins in Cr_2O_3 are easily reoriented even at temperatures much lower than T_N , as was revealed in Ref. [160]. This behavior of the spins extends the range of the Heisenberg type of critical behavior and shifts the crossover temperature ε_{cr} to the Néel point. Therefore, the entire above-considered range of reduced temperatures can correspond to the Heisenberg type of critical behavior.

The values of α slightly lower than those predicted by the theory [6–8] and found in experiments [189, 190] also seem to be related to the presence of a substantial portion of weakly bound surface spins (22.8–46.8%). Note that in treating the data on the low-temperature phase ($T < T_N$) without regard for the scaling assumption $\alpha' = \alpha$ we arrived at $\alpha' \approx 0.03(3)$ in the temperature range studied. In this case the ratio between A and A' varies from 2.0 to 5.0.

To study the critical behavior of particles in more detail, we should consider the temperature dependences of the sublattice magnetization m and susceptibility χ . Note right away that both the quantities are unsuitable for study by the MC methods, since the magnetization m has high-temperature ‘tails’ near T_N , and χ fluctuates greatly.

Figure 9a demonstrates the temperature dependence of magnetization m for two particles with $N = 508$ and $N = 2170$. Noteworthy are the residual values of the magnetization typical of the MC data, which noticeably decrease as N rises.

To approximate the critical behavior of the sublattice magnetization m , we used the expression

$$m = B|\varepsilon|^\beta(1 + a_m|\varepsilon|^\chi), \quad (5.6)$$

where B and a_m are the critical amplitude and the scaling correlation amplitude respectively. Table 4 lists the data on β at $a_m \neq 0$ and $a_m = 0$ in the temperature range $\varepsilon_{\text{min}} \leq \varepsilon \leq \varepsilon_{\text{max}}$. Note that the exponent β , unlike other exponents studied (α and γ), depends on the number of spins in the particle. Its absolute value increases with increasing N .

Table 4. Effective values of the critical exponent β for small magnetic particles ($\varepsilon_{\text{min}} \leq \varepsilon \leq \varepsilon_{\text{max}}$, $\varepsilon_{\text{max}} = 0.75$).

N	$a_m = 0$				$a_m \neq 0$			
	ε_{min}				ε_{min}			
	5×10^{-3}	1×10^{-2}	3×10^{-2}	8×10^{-2}	1×10^{-2}	3×10^{-2}	8×10^{-2}	
286	0.18	0.21	0.26	0.31	—	—	—	
508	0.22	0.25	0.29	0.32	0.23	0.28	0.34	
760	0.25	0.27	0.30	0.33	0.25	0.30	0.36	
908	0.25	0.31	0.32	0.36	0.26	0.31	0.38	
1602	0.29	0.31	0.33	0.36	0.28	0.32	0.38	
2170	0.33	0.37	0.39	0.41	0.30	0.35	0.39	
2502	0.33	0.37	0.40	0.43	0.30	0.34	0.40	

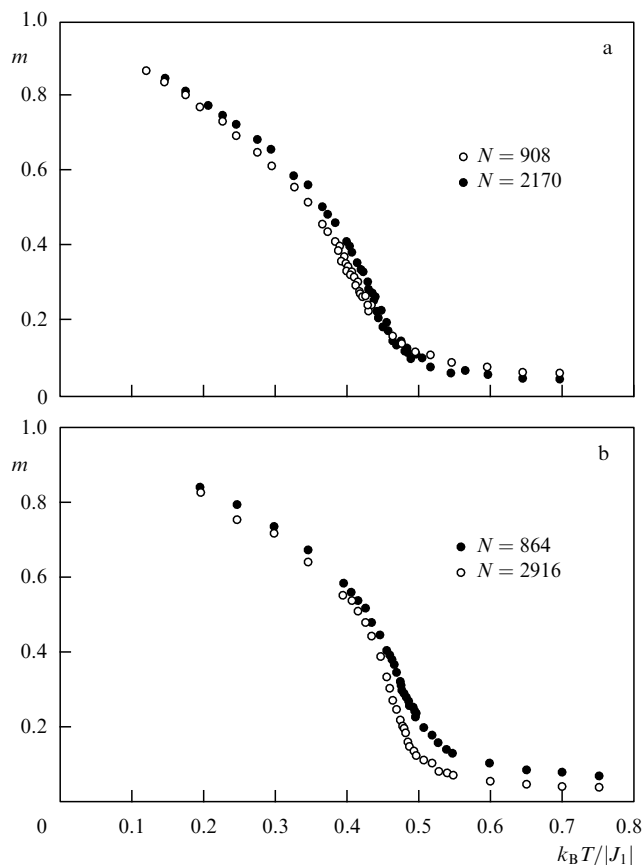


Figure 9. Dependence of the sublattice magnetization m on the temperature $k_B T/|J_1|$ in the antiferromagnetic Cr_2O_3 model: (a) small particles [185], and (b) systems with periodic boundary conditions (model I).

One more tendency is observed for β : it likewise increases with increasing ε_{\min} . These features seem to be related to the short-order effects, which are indicated by high-temperature tails of magnetization shown in Fig. 9a. The dependence $m(\varepsilon)$ depicted in the double-logarithmic scale shows a bend at $\varepsilon_B \approx 0.08$. Figure 10a plots typical temperature dependences with $\beta \approx 0.27$ at $\varepsilon \leq \varepsilon_B$ and $\beta \approx 0.38$ at $\varepsilon > \varepsilon_B$ for a particle

containing $N = 1602$ spins. These data may suggest a cross-over from the Heisenberg behavior at $\beta \approx 0.38$ (more precisely, $\beta = 0.367$ in the Heisenberg model) to the Ising behavior with $\beta \approx 0.27$ ($\beta = 0.326$ in the Ising model [6–8]), which is not observed in the temperature dependence of heat capacity.

Typical temperature dependences of the susceptibility obtained by (5.3) are plotted in Fig. 8a. To treat them, we use the relation

$$\chi = \Gamma |\varepsilon|^{-\gamma}, \quad (5.7)$$

where γ and Γ are, respectively, the critical exponent and amplitude for the susceptibility. Table 5 lists the data on γ obtained by (5.7). The critical exponents γ and γ' were found independently, below and above the critical temperature T_N , which was calculated from the maximum of the susceptibility χ . The critical exponents γ and γ' as well as α are independent of the number of spins in the particle. But the values of γ and γ' depend strongly on ε_{\min} , and increase as ε_{\min} grows. Note that the absolute values of γ and γ' do not enable one to decide the type of the critical behavior of susceptibility to be either Ising ($\gamma = 1.24$) or Heisenberg ($\gamma = 1.39$).

Table 5. Effective values of the critical exponents γ and γ' for small magnetic particles ($\varepsilon_{\max} = 0.75$).

N	γ		γ'			
	ε_{\min}		ε_{\min}			
	4×10^{-2}	8×10^{-2}	1×10^{-1}	4×10^{-2}	8×10^{-2}	1×10^{-1}
508	0.96(3)	1.14(3)	1.22(3)	0.90(3)	1.15(3)	1.33(3)
760	0.94	1.15	1.20	0.93	1.14	1.30
908	1.02	1.14	1.18	0.91	1.22	1.31
1602	1.01	1.15	1.19	0.90	1.21	1.30
2170	1.00	1.13	1.20	0.95	1.20	1.28
2502	0.98	1.13	1.22	0.96	1.18	1.29

5.2 Phase transitions and critical phenomena in macrosystems

Let us consider the critical behavior of Cr_2O_3 macrosystems on which periodic boundary conditions are imposed. It is well known that in finite-size systems there are no genuine phase

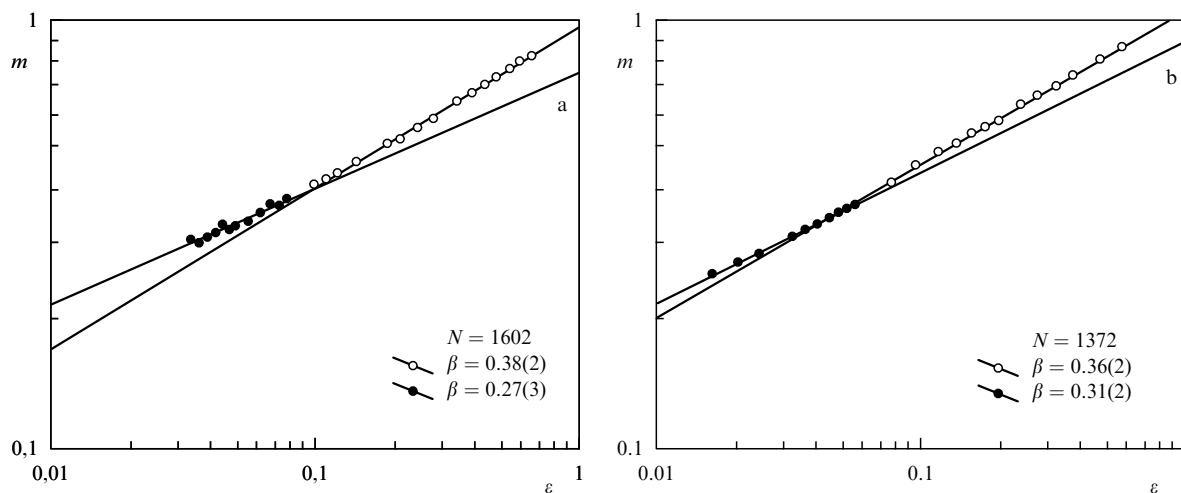


Figure 10. Double-logarithmic dependence of the sublattice magnetization m on the reduced temperature ε in the antiferromagnetic Cr_2O_3 model: (a) small magnetic particle, and (b) system with periodic boundary conditions (model I).

transitions; therefore, the most serious drawback of the numerical simulation of PT and CP is that one has to deal with a finite number of particles N . As a result, the region of the phase space for which the partition function is calculated has a finite size and the thermodynamic functions are regular. Nevertheless, finite-size systems allow one to reveal many essential features of phase transitions. The study of such pseudotransitions and their behavior in relation to the size of the system provides valuable information on PT in infinite systems. We will consider the potential of the MC method and the peculiarities of PT and CP by examining the antiferromagnetic Cr_2O_3 model.

From our standpoint, it is necessary to consider the following values of the ratio between the anisotropy D_0 and the exchange J_1 in Hamiltonian (5.1):

$D_0/|J_1| = 2.5 \times 10^{-4}$, which corresponds to Cr_2O_3 samples [182, 183]; and

$D_0/|J_1| = 2.5 \times 10^{-2}$, which is typical of small magnetic systems with uniaxial anisotropy and sizes up to several angstroms [192, 193].

Below, we will refer to the first case as to *model I*, and to the second case, as to *model II*. All the crystallographic, exchange, and other data used in model I correspond to real Cr_2O_3 samples. In model II, the value of the anisotropy constant D_0 is taken to correspond to small magnetic particles, since despite the periodic boundary conditions the systems modeled by MC have finite linear sizes $L \ll \infty$ ($L \sim N^{1/3}$), and therefore may exhibit some properties typical of small systems.

The MC calculations were performed for systems with periodic boundary conditions using the conventional Metropolis algorithm [10]. The studied systems included $N_{\text{ef}} = 500, 864, 1372, 2048, 2916$, and 4000 spins. To equilibrate the systems, we ignored in each system a portion of the Markovian chain of length up to 3×10^4 , which was several times larger than the nonequilibrium portion. Then we averaged over the whole equilibrium portion of length 12×10^5 . To control the accuracy of the results obtained, we repeated the experiments with portions of double length. The latter did not affect the accuracy of the calculations.

Figures 7b and 8b present the temperature dependences of C and χ . Note that the temperature dependences of C and χ have pronounced maxima as in the case with Cr_2O_3 particles, but the positions of the maxima coincide for systems containing different numbers N_{ef} of spins within the accuracy of calculations, which suggests that the chosen way of imposing periodic boundary conditions well offset the boundary effects. One can only see a pronounced increase in the maxima, which takes place as the number of spins in the system increases. Figure 9b plots the temperature dependence of the sublattice magnetization m for two systems with $N_{\text{ef}} = 864$ and $N_{\text{ef}} = 2916$. Note that m decreases monotonically and the effects related to the finite number of spins N in the system decay noticeably as N_{ef} rises. The critical temperature T_N calculated from the data presented in Figs 7–9 has a large scatter.

To determine the critical temperature, we used the Binder cumulants considered in Section 3. Figure 2 demonstrates the temperature dependence of the fourth-order Binder cumulant U_L for model I. The maximum slope of the dependence can serve as an estimate of the effective temperature of phase transition. This method can also be applied to systems of different sizes L , in order to determine the phase transition temperature. The point is that the cumulants for systems of all

sizes should cross at $T = T_c$ provided that the calculations are performed with care. All the details of determining T_c in the above-discussed way were studied in Refs [128, 146] as applied to the ferromagnetic Ising and Heisenberg models with the interaction between the nearest neighbors.

The values of T_N calculated for models I and II in the above-discussed way are equal to $T_N = 0.466(5)$ and $T_N = 0.480(5)$, respectively. We used them as the critical ones. Some increase in the transition temperature for model II which takes place as anisotropy grows is consistent with the well known fact of a higher value of T_c in the Ising systems as compared to that in the Heisenberg models. In what follows, we will see once again that the anisotropy value $D_0/|J_1| = 2.5 \times 10^{-2}$ used in model II leads to predominance of the Ising critical behavior of the model under study and tells on the values of all critical parameters.

The calculated data on heat capacity were approximated by (5.4) and (5.5). In this case too, the use of (5.5) decreased the error of calculations. Table 6 lists the data obtained on α , A , A' for the models I and II (to calculate A' at $T < T_N$, we used the equilibrium scaling theory $\alpha' = \alpha$ [1]). All the values of α in model I are negative and, as is typical of the Heisenberg model, virtually do not depend on the number of spins in the systems, and agree well with the theoretical estimate $\alpha = -0.126(28)$ obtained in the isotropic Heisenberg model with short-range forces [6–8]. The ratio between the critical amplitudes A and A' derived in the above discussed way vary over the range $0.90 \leq A/A' \leq 1.10$ for all the systems. The picture changes significantly for model II, where the values of α are positive, which is specific to the Ising model. A theoretical estimate of α for the Ising model obtained by the ε expansion is equal to $\alpha = 0.108(9)$ [6–8]. A relatively large value of anisotropy of single ions, which is typical of small magnetic particles [192, 193] and used by us in model II, provides that the systems with periodic boundary conditions behave as the Ising ones. Note that the systems with free boundaries behave as Heisenberg ones at the same anisotropy [185, 186]. The ratio between the amplitudes varies over the range $0.75 \leq A/A' \leq 0.9$ for model II.

Table 6. Effective values of critical exponent α and the critical amplitudes A and A' ($5.0 \times 10^{-3} \leq \varepsilon \leq 7.5 \times 10^{-1}$).

N	$D_0/ J_1 = 2.5 \times 10^{-4}$			$D_0/ J_1 = 2.5 \times 10^{-2}$		
	α	A	A'	α	A	A'
500	-0.15(3)	0.61(2)	0.60(2)	0.11(3)	0.53(3)	0.70(3)
864	-0.15	0.56	0.56	0.12	0.43	0.61
1372	-0.16	0.51	0.49	0.10	0.44	0.57
2048	-0.12	0.47	0.46	0.13	0.44	0.52
2916	-0.15	0.53	0.53	0.10	0.38	0.42
4000	-0.14	0.47	0.48	0.15	0.42	0.43

As $\varepsilon \rightarrow 0$, the system is expected to exhibit a crossover from the Heisenberg behavior to the Ising one [191]. The theoretical estimate of the crossover temperatures calculated from our data are equal to $\varepsilon_{\text{cr}} \approx 0.0013$ and $\varepsilon_{\text{cr}} \approx 0.052$ for models I and II, respectively. The data on α obtained in model I do not suggest the occurrence of the crossover in the range $5 \times 10^{-3} \leq \varepsilon \leq 7.5 \times 10^{-1}$. As for model II, it behaves as an Ising one at all the temperatures studied.

Let us consider the temperature dependences of the sublattice magnetization m and susceptibility χ . As is seen from Fig. 9b, the magnetization m decreases monotonically as the temperature rises, and differs from zero even at tempera-

Table 7. Effective values of the critical exponent β ($\varepsilon_{\max} = 7.5 \times 10^{-1}$).

N	$D_0/ J_1 = 2.5 \times 10^{-4}$					$D_0/ J_1 = 2.5 \times 10^{-2}$				
	ε_{\min}					ε_{\min}				
	5×10^{-3}	1×10^{-2}	2×10^{-2}	4×10^{-2}	8×10^{-2}	5×10^{-3}	1×10^{-2}	2×10^{-3}	4×10^{-2}	8×10^{-2}
500	0.24(3)	0.25	0.26	0.28	0.28	0.18	0.21	0.23	0.24	0.25
864	0.25	0.26	0.27	0.29	0.29	0.20	0.23	0.24	0.25	0.26
1372	0.27	0.29	0.32	0.35	0.36	0.21	0.24	0.25	0.26	0.27
2048	0.28	0.28	0.32	0.33	0.34	0.21	0.24	0.25	0.26	0.28
2916	0.31	0.34	0.35	0.36	0.37	0.25	0.26	0.27	0.29	0.30
4000	0.33	0.35	0.36	0.38	0.38	0.27	0.27	0.28	0.29	0.31

tures far above the critical one T_c . To approximate the critical behavior of m , we used (5.6). Table 7 lists the data on β obtained for various temperature ranges of ε . Note that the values of β are slightly higher for model I than for model II in the same temperature range. In both the models, the exponent β exhibits the same behavior as in small magnetic particles, i.e., it rises as N_{ef} and ε_{\min} grow.

We believe both the features to result from short-order effects (Fig. 9b).

The dependence of the sublattice magnetization m on the reduced temperature ε in model I presented in the double-logarithmic scale shows a bend, which is typical of the crossover behavior. Figure 10b depicts this dependence at two values of $\beta \approx 0.31(2)$ at $\varepsilon \leq \varepsilon_{\text{cr}}$ and $\beta \approx 0.36(2)$ at $\varepsilon > \varepsilon_{\text{cr}}$ for a system containing $N_{\text{ef}} = 1372$ particles. A similar effect is observed in model I for the systems of all sizes studied. Probably, these data suggest that the critical behavior of model I changes from the Heisenberg type at $\beta \approx 0.36$ (the exact theoretical value is $\beta = 0.367$ [6–8]) to the Ising type at $\beta \approx 0.31$ (the theoretical estimate is $\beta = 0.326$ [6–8]), which is not observed for heat capacity.

A similar $m(\varepsilon)$ dependence for model II does not show any peculiarities typical of model I, and the values $\beta \approx 0.30(2)$ obtained for this model are rather close to the theoretical estimate for the Ising model.

The experimental value of β obtained for Cr_2O_3 in the temperature range $3 \times 10^{-5} \leq \varepsilon \leq 3 \times 10^{-2}$ is equal to $\beta = 0.35$ [194] and close to that for the Heisenberg model and to the value obtained by us in model I with the Heisenberg behavior.

Figure 8b plots the typical temperature dependences of χ . To approximate them, we used (5.7). Table 8 lists the data on γ and γ' obtained in model I. These values were calculated independently above and below the critical temperature T_N . Note that these exponents as well as α , are independent of the number N_{ef} of spins in the system studied, and increase as ε_{\min} increases. Using these values, we cannot identify the type of critical behavior as Heisenberg ($\gamma = 1.39$) or Ising ($\gamma = 1.24$)

[6–8]. Similar data obtained in this way for model II coincide with the data listed in Table 8 within the accuracy of calculations. The behavior of γ and γ' may probably be attributed to the fact that the resolution of the procedure is not sufficient to treat the intensely fluctuating susceptibility. In the next section, we will show that the analysis of the same data by another method provides a clearer idea of the critical behavior of susceptibility.

The results we have been discussing in this section were obtained by approximating the MC data with traditional step functions. We shall now consider an analysis of the same data based on the theory of finite-size scaling.

5.3 Finite-size scaling and critical exponents of models of real magnets

Finite-size systems can be used to model infinite systems as long as the correlation length ξ does not exceed the linear size L of the system. When near the critical point $\xi \geq L$, the critical properties of systems depend strongly on the type of periodic boundary conditions. Due to fluctuations, the critical properties can be revealed in a temperature range below and above the critical point, but the latter cannot exist in real systems. As a result, ‘rounding’ effects such as long-range ordering above the critical temperature, smoothing out of heat capacity and susceptibility peaks and their temperature shift, etc. take place. The first theory where the influence of finite sizes on the critical phenomena was taken into account was developed by Ferdinand and Fisher [195, 196]. Most fully the finite-size scaling (FSS) theory is presented in Ref. [96]. The ideas underlying the theory enable one to extrapolate the MC data obtained for finite-size systems to the thermodynamic limit ($N = L^3 \rightarrow \infty$) and are widely used [119, 120, 128, 147, 148]. According to the theory, the free energy of a rather large system with periodic boundary conditions at temperature T close to the critical temperature T_c of the infinite system can be presented as

$$F(T, L) \sim L^{-d} F_0(\varepsilon L^{1/\nu}), \quad (5.8)$$

Table 8. Effective values of the critical exponents γ and γ' for a system with periodic boundary conditions ($\varepsilon_{\max} = 0.75$, $D_0/|J_1| = 2.5 \times 10^{-4}$).

N	γ				γ'			
	ε_{\min}				ε_{\min}			
	1×10^{-2}	2×10^{-2}	4×10^{-2}	8×10^{-2}	1×10^{-2}	2×10^{-2}	4×10^{-2}	8×10^{-2}
500	0.86	1.05	1.08	1.17	0.92	1.07	1.15	1.29(4)
864	0.87	1.07	1.10	1.17	0.93	1.08	1.20	1.31
1372	0.89	1.09	1.13	1.19	0.94	1.10	1.15	1.32
2048	0.90	1.11	1.15	1.21	0.96	1.12	1.19	1.31
2916	0.89	1.10	1.11	1.18	1.03	1.14	1.21	1.34
4000	0.93	1.12	1.17	1.23	1.03	1.15	1.22	1.33

where $\varepsilon = |T - T_c|/T_c$, $T_c = T_c(L = \infty)$, and ν is the equilibrium critical exponent of the correlation radius of the infinite system ($L = \infty$). The shift of the effective temperature of the phase transition caused by changes in sizes of the system is expressed as

$$\frac{k_B T_c(L)}{J} = \frac{k_B T_c}{J} + aL^{-1/\nu}, \quad (5.9)$$

where a is a constant. Equation (5.8) leads to similar equations for the heat capacity, spontaneous magnetization, and susceptibility per spin [119]

$$C(T, L) \sim L^{\alpha/\nu} C_0(\varepsilon L^{1/\nu}), \quad (5.10)$$

$$m(T, L) \sim L^{-\beta/\nu} m_0(\varepsilon L^{1/\nu}), \quad (5.11)$$

$$\chi(T, L) \sim L^{\gamma/\nu} \chi_0(\varepsilon L^{1/\nu}), \quad (5.12)$$

where α , β , and γ are the equilibrium exponents for the system at $L = \infty$. They are related by the hyperscaling equation $2 - \alpha = d\nu = 2\beta + \gamma$ [4].

Equations (5.10)–(5.12) adequately reproduce the critical behavior of infinite systems at $\varepsilon \ll 1$ and $L \rightarrow \infty$. The validity of the finite-size scaling theory was shown by the MC study of the 2d and 3d Ising models both with periodic boundary conditions and with free boundaries [91, 92, 119, 120]. The application of (5.10)–(5.12) to the MC data should remove finite-size effects. To what extent the relations of the FSS theory are suitable to treat our data can be inferred from Fig. 11, where the scaled data for model II are plotted. The data obtained for model I are scaled in a similar manner. The FSS relations are equally effective to study heat capacity and magnetization for both models.

According to the theory, in the system of size $L \times L \times L$ at $T = T_N$ and large L , the magnetization and susceptibility

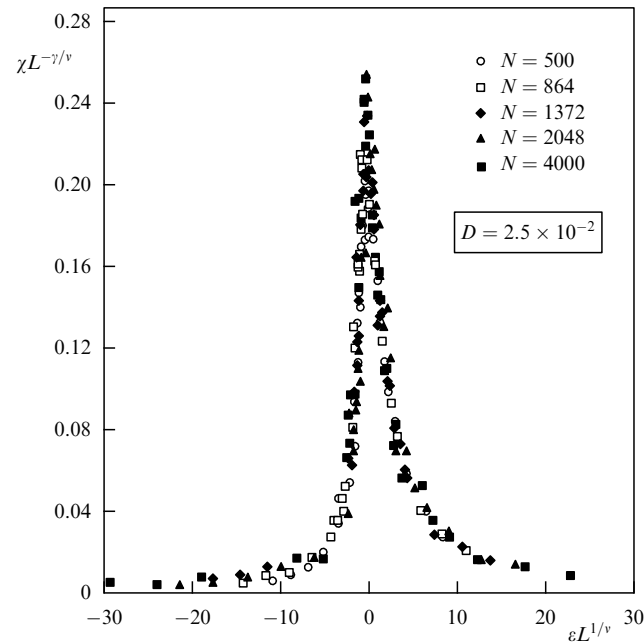


Figure 11. Data on the susceptibility of Cr_2O_3 samples, scaled by (5.12) for the model II.

satisfy the following relations:

$$m \sim L^{-\beta/\nu}, \quad (5.13)$$

$$\chi \sim L^{\gamma/\nu}. \quad (5.14)$$

Treating our data using (5.13) and (5.14), we also obtained the values of β and γ . For this purpose, we plotted the dependences of m and χ on the lattice size L on the double-logarithmic scale (Figs 12 and 13). All the points of the curves fall on a straight line within the accuracy of calculations. Note that even in the system of the smallest size $L \approx 8$, the arrangement of the points does not drop out of the general pattern. The asymptotic finite-size scaling behavior seems to take place even at $L \geq 8$. The dependences plotted in Figs 12 and 13 were derived with the use of the least-squares method. The slope of the straight line determines the values of β/ν and γ/ν , which are equal to 0.544 and 1.985 for model I. Taking into account that model I has a clearly pronounced Heisenberg character and $\nu = 0.706$ [6–8], we have $\beta = 0.38(2)$ and $\gamma = 1.38(2)$. Note that these values are in agreement with the theoretical estimates for the Heisenberg model ($\beta = 0.368$, $\gamma = 1.39$ [6–8]). In model II, we have $\beta/\nu = 0.426$ and $\gamma/\nu = 1.791$. Since this model exhibits Ising behavior, while the initial Hamiltonian shows Heisenberg behavior, we determine the exponents at both $\nu = 0.706$ (Heisenberg model) and $\nu = 0.63$ (Ising model). Thus, we have $\beta = 0.30(2)$, $\gamma = 1.26(3)$ at $\nu = 0.706$, and $\beta = 0.27(2)$, $\gamma = 1.13(3)$ at $\nu = 0.63$. The values obtained for model II are

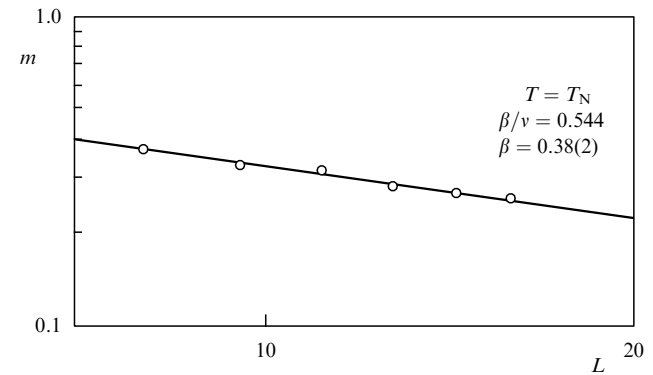


Figure 12. Double logarithmic dependence of the magnetization m on the reduced temperature ε , obtained for Cr_2O_3 samples (model I).

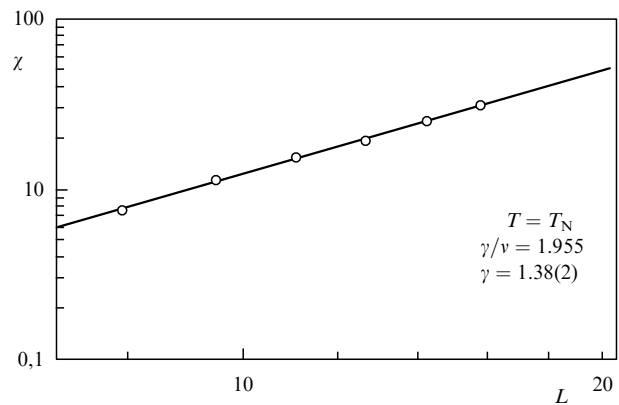


Figure 13. Size dependence of the susceptibility $\chi(L)$ at $T = T_N$ for Cr_2O_3 samples (model I).

close to the theoretical estimates for the Ising model ($\beta = 0.326$, $\gamma = 1.24$ [6–8]) and are slightly less at $\nu = 0.63$.

In the case of sharply peaked heat capacity curve, the scaling of C_{\max} is usually performed by [128, 197]

$$C_{\max}(L) = C_{\max}(L = \infty) - aL^{\alpha/\nu}, \quad (5.15)$$

where a is a constant (Fig. 14). Approximation of the data by (5.15) yields the critical exponent $\alpha = -0.14(3)$ for model I, and $\alpha = 0.16(3)$ at $\nu = 0.706$ and $\alpha = 0.14(3)$ at $\nu = 0.63$ for model II. These results agree well with the theoretical estimates obtained for the Heisenberg ($\alpha = -0.126$ [6–8]) and the Ising ($\alpha = 0.108$ [6–8]) models and with the data calculated by the MC data treated by the conventional power dependences.

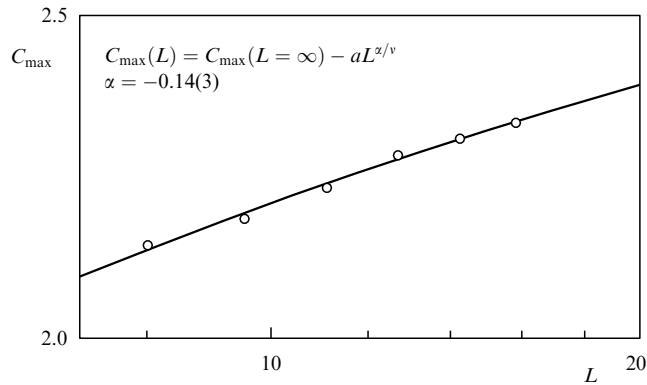


Figure 14. Size dependence of heat capacity maximum $C_{\max}(L)$ for Cr_2O_3 samples (model I).

Our data obtained by the MC study of models of real antiferromagnetic Cr_2O_3 suggest that model I with weak anisotropy behaves as the Heisenberg one under the conditions studied. The critical exponents α for heat capacity derived from the power dependences and finite-size scaling relations are in good agreement and correlate well with the theoretical estimates.

The exponents β and γ calculated in the conventional way with the use of (5.6) and (5.7) show features typical of MC data and cannot be used to identify the type of critical behavior. The values of α , β , and γ obtained by the FSS treatment of the same data suggest that model I behaves as the Heisenberg one with critical exponents $\alpha = -0.14(3)$, $\beta = 0.38(2)$, and $\gamma = 1.38(2)$.

The analysis of the data obtained at $D_0/|J_1| = 2.5 \times 10^{-2}$ (model II) and treated by both the methods proves the model II to exhibit Ising critical behavior.

Note that, although the values of critical exponents α , β and γ found by the FSS theory are in better agreement with the theoretical estimates and experimental results, approximation of the same data by conventional power functions yields a great body of additional information. We believe that to gain a comprehensive idea of the critical behavior of the systems under study, the results of the MC modeling should be analyzed by both the methods.

6. MC study of the dynamic critical behavior

The investigation of the dynamic properties of condensed systems near the critical points is a traditional concern of

statistical physics. Development of a complete theory of dynamic critical phenomena on the basis of microscopic Hamiltonians is a central problem of the modern theory of PT and CP, which is still far from being solved. Nevertheless, the available analytical approaches based on the RG approach [2], the theory of interacting modes [4], and dynamic scaling [2, 4] start from microscopic Hamiltonians in considering spin systems. Note that theoretical and experimental studies in this field run into severe difficulties [198–205]. Nevertheless, noteworthy is the most essential step forward yet taken in this direction, which is the application of the RG method and the ϵ expansion to the study of dynamic critical phenomena [198, 199]. It has enabled the calculation of the dynamic critical exponent z (Table 9) for some particular models and to reveal the main effects influencing its numerical values. The analysis of dynamic critical phenomena demonstrates that the exponent z is one of the main characteristics of the critical dynamic behavior. It has turned out to depend not only on the space dimension d , the number n of degrees of freedom of the order parameter, and the type of ordering interaction, but also on the conservation of the characteristic energy and the order parameter. The main expression of the dynamic scaling, which determines this critical exponent, takes on the form [1]

$$\omega = q^z f(q\xi_c), \quad (6.1)$$

where ω is the characteristic frequency of fluctuations with wave number q , and ξ_c is the critical correlation radius.

The dynamic critical properties of magnetically ordered materials, especially ferromagnets, are highly diversified and complicated, since account should be taken not only of the strong exchange interactions but also of the weak relativistic ones. The most significant of the latter are the dipole interactions, which grow in importance as the system approaches the critical point. As a result, the critical region turns out to be divided into two regions, in one of which the dipole effects are dominant, while in the other, exchange

Table 9. Theoretical estimates of the dynamic critical exponent z .

Spin system model	Universality class for equilibrium critical behavior	Scaling law	Approximated numerical values at $d = 3$
Model A. Anisotropic magnets, where the order parameter and the energy are not conserved	(1, d)	$z = 2 + c\eta$, $c = 6 \ln(4/3) - 1$	2
Model C. Anisotropic magnets, where the order parameter is not conserved, while the energy is conserved	(1, d)	$z = 2 + \alpha/\nu$, $n = 3$; $z = 2 + 2\alpha/n\nu$, $0 < n \leq 2$; $z = 2, n \geq 4$	2
Model G. Anisotropic antiferromagnets	(3, d)	$z = d/2$	3/2
Model J. Isotropic antiferromagnets	(3, d)	$z = (d + 2 - \eta)/2$	5/2
Ferromagnets with a dipole interaction: normal and rigid dynamics	(3, d)	$z = 2 - \eta$,	2
		$z = 2 + c\eta$,	2
		$c = 0.94$; $z = (5 - \eta)/2 - 1/\nu$	1

forces prevail [200–202]. According to the experiments on ferromagnets, in the region with prevailing exchange forces the predictions of the theory of interacting modes and dynamic scaling are correct [200–203]. In the region with dominant dipole interactions the theory predicts two types of behavior, i.e., normal and rigid. These experimental data are contradictory and cannot be treated in a unique manner [200–204]. The considerable difficulties encountered in the theoretical and experimental studies have not yet been overcome. We believe that the MC methods, which in recent years have been intensively applied to study dynamic critical phenomena, would clarify at least some of the significant questions concerned. Note that the main advantage of the MC treatment is that all the parameters affecting the physical processes are controlled.

The MC study of various aspects of dynamic properties of the Heisenberg and Ising models has received considerable attention [160, 161, 205–226]. Quantitative studies of the critical dynamics by the MC method have started only recently, and they are fewer in number than those dealing with the equilibrium dynamic properties. In recent years a number of works have appeared, where various MC versions were used to investigate dynamic properties near T_c and calculate the critical exponent z [208, 211, 213–220, 226]. The values of the critical exponent z for the Ising model obtained in earlier works show a wide scatter from 2.17 [222] to 1.95 [225]. These studies demonstrate the tendency for the exponent z to decrease as the size of the system under consideration and the duration of calculations rise. The latter seems to result from the finite-size effects and/or insufficient data considered in statistical treatment. Some results obtained with the use of supercomputers and powerful special-purpose computer complexes on large-size lattices ($L \times L \times L$, $L = 512$) yield $z = 1.95$ [223] and $z = 1.99$ [226] for the 3d Ising model. Despite the high accuracy of the calculations, these values do not agree with the lowest estimate $z = 2$ predicted by the ε expansion for all the systems with the space dimensionality varying from 1 to 4 [227].

An attempt to clarify the situation with contradictory z values was made in Refs [207, 208]. The authors of Ref. [208] analyzed possible systematic errors arisen in the MC study of dynamic properties. They investigated the time correlation functions $\Phi(t)$ for the magnetization and the energy at T_c on SC lattices of size $L \times L \times L$, $L \leq 96$ with periodic boundary conditions. The time correlation functions $\Phi_A(t)$ for a thermodynamic value A were shown to be calculated as

$$\Phi_A(t) = \frac{\langle A(0)A(t) \rangle - \langle A(0) \rangle \langle A(t) \rangle}{\langle A(0)A(0) \rangle - \langle A(0) \rangle \langle A(0) \rangle} \quad (6.2)$$

under the condition that the number of MC steps tends to infinity ($N \rightarrow \infty$). In the general case, the function $\Phi_A(t)$ is written [228, 229] as

$$\Phi_A(t) = \sum_i a_i \exp\left(-\frac{t}{\tau_i}\right), \quad (6.3)$$

where a_i are unknown coefficients. Using the nonlinear least-squares method to treat $\Phi_A(t)$, we obtain τ_i values, which can be considered as the relaxation times for the system studied. To find τ_i , the authors of Ref. [208] calculated the time correlation functions for the energy E on the time interval t of length up to $t = 1000$ MC steps/spin and the time correlation functions for the magnetization M on the time interval t of length up to $t = 5000$ MC steps/spin. The

corresponding relaxation times were also evaluated in Ref. [211] for the classical Heisenberg model on an SC lattice at $t = 3000$ MC steps/spin. There, $\Phi(t)$ was approximated by both the ordinary exponent $\sim A[\exp(-t/\tau)]$ and a two-exponent function:

$$\Phi(t) = a_1 \exp\left(-\frac{t}{\tau_1}\right) + a_2 \exp\left(-\frac{t}{\tau_2}\right). \quad (6.4)$$

It turned out that the values τ_i calculated using the simple exponent are less by several percent than those obtained by (6.4). In Ref. [230] the critical exponent z is determined by finite-size scaling. Following the theory, in the dynamic critical region the relaxation time τ is scaled as

$$\tau(\xi, L, \varepsilon) = L^z f\left(\frac{\xi}{L}, \varepsilon L^{-z}\right), \quad (6.5)$$

where ξ is the correlation length, and $f(x, y)$ is the scaling function. At the point T_c the characteristic scale is determined by the linear size L of the system, and the relaxation time is defined as $\tau \sim L^z$ at asymptotically large $L \rightarrow \infty$.

For the Ising model, the critical exponent z obtained by the $\Phi_M(t)$ dependences for lattices of size $L \geq 12$ is equal to 2.04 ± 0.03 , which is in good agreement with the ε expansion value $z = 2.02$ [199]. The data obtained by the study of $\Phi_E(t)$ are less accurate and yield $z = 2.03 \pm 0.10$.

It is pertinent to consider some methodological points. As is shown in Ref. [208], a system with $L \leq 12$ exhibits deviations from the asymptotic behavior and the FSS analysis should be improved. Investigation of the system with $L = 12$ shows that the relaxation times can be affected by the type of periodic boundary conditions, although the effect probably decreases as L rises. These facts suggest that the dynamic critical phenomena are difficult to study not only by the theoretical and experimental methods but also by numerical calculations.

Figure 15 plots typical data obtained by this way for the Heisenberg model [211] on SC lattices within the approach discussed. The estimate $z = 1.96(6)$ is obtained from the data

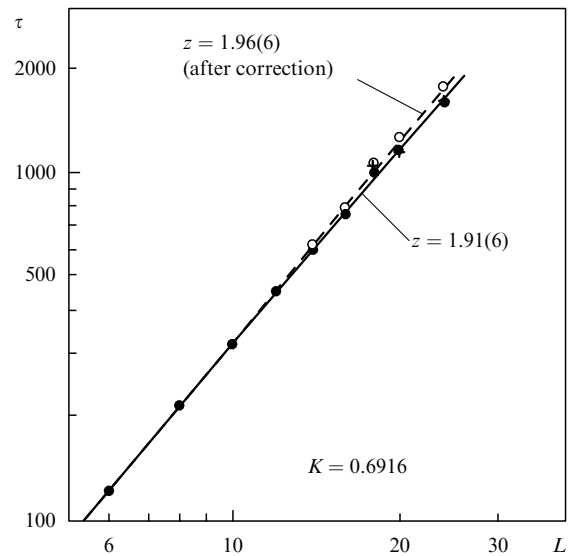


Figure 15. Double-logarithmic dependence of the relaxation time τ for magnetization on the lattice size L obtained in the 3d Heisenberg model at $T = T_c$ ($K_c = J/k_B T_c = 0.6929$) [211].

shown in the figure after the use of a correcting procedure described in Ref. [211] (Fig. 15, dashed line). This value z differs slightly from that found by the RG theory [231–233]:

$$z = 2 + c\eta, \quad c = 6 \ln \left(\frac{3}{4} \right) - 1; \quad (6.6)$$

which yields $z \approx 2.024$. But the estimate by the MC data is in agreement with the prediction of the classical theory of critical retarding $z = 2 - \eta$ [234, 235]. The authors of Ref. [211] explain the difference between the MC and RG results by the fact that the MC data are systematically shifted, for example, due to the narrow range of L variation (from 6 to 24). Another possible reason indicated in Ref. [208] is the finite number of MC steps; this error cannot be ignored even given considerable MC statistics.

For the Heisenberg model, various experimental data yield $1.88 - 2.09$ including a high error (± 0.05) of measurements. These data agree with the theory only qualitatively and do not clarify the situation.

A direct comparison of the MC data with experimental results is rather difficult, since the ‘artificial’ stochastic dynamics used in the MC process results in purely relaxation behavior. Note also that recent experiments on the critical behavior of isotropic ferromagnets (EuO, EuS) have revealed a crossover from $z \approx 2.5$ to $z \approx 2.0$, which is probably explained by the presence of dipole–dipole interactions [211].

The critical exponent z can also be estimated from the dependence of the relaxation time on the closeness to the critical temperature [199]. If the correlation length ξ diverges as $\xi \sim [(T - T_c)/T_c]^{-\nu} = (\varepsilon)^{-\nu}$ at T_c , then this dependence of the relaxation time is expressed as

$$\tau \sim \left(\frac{T}{T_c} - 1 \right)^{-\theta}, \quad (6.7)$$

where $\theta = zv$. Figure 16 depicts a typical finite-size scaling dependence $\tau(\varepsilon)$ for the $3d$ Heisenberg model on an SC lattice, which is derived from

$$\tau_L(\varepsilon) = L^z f(\varepsilon L^{1/\nu}). \quad (6.8)$$

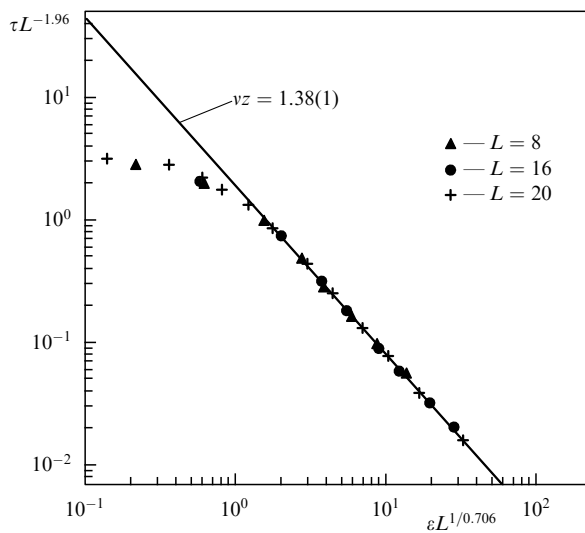


Figure 16. Double-logarithmic dependence of the relaxation time τ on the reduced temperature ε obtained in the $3d$ Heisenberg model treated by FSS analysis in the paramagnetic range $K_c = J/k_B T_c = 0.6929$ [211].

The values $\theta = 1.28$ [208] and $\theta = 1.38$ [211] calculated for the Heisenberg and the Ising models are best suited to describe the experimental MC data. Using $\nu = 0.63$ and $\nu = 0.706$ for the Ising and Heisenberg model, respectively, we arrive at $z = 2.03$ and $z = 1.95$. For the Heisenberg model the value $\theta = 1.38(1)$ not only coincides with that predicted by the RG method $\theta = 1.38(5)$, but also surpasses it in accuracy. Note that the values obtained by the size dependences of τ agree well with those derived from the temperature dependences of τ for both the models. The authors of Ref. [208] point out that the first method provides higher accuracy of z calculation than the second one and discuss various reasons for the difference between the theoretical data and the results found by other authors.

In recent years, much attention has been given to studies aimed at elucidation of the extent of influence of impurities and other nonideal properties of real crystals on the critical behavior of systems at phase transitions [107]. For instance, it was found [236] that the presence of impurities changes the critical properties of magnets whose heat capacity diverges at T_c . The RG method showed [237, 238] that the critical behavior of the dilute Ising model can be assigned to a new universality class, and the critical exponents do not depend on the concentration of point impurities until it exceeds a threshold value. In this regard, the works of Prudnikov and his associates concerned with the critical dynamics of dilute Ising systems are very interesting. The $3d$ Ising model of size $L \times L \times L$ ($L = 48$) is considered in [213, 214] at various spin concentrations $p = 1.0, 0.95, 0.8, 0.6$, and 0.4 . In Ref. [224], the MC method is combined with the dynamic RG approach to calculate the critical exponent z . There, the concentration dependence of the critical exponent $z(p)$ was found: $z(1.0) = 1.98 \pm 0.08$, $z(0.95) = 2.19 \pm 0.07$, $z(0.8) = 2.20 \pm 0.08$, $z(0.6) = 2.58 \pm 0.09$, and $z(0.4) = 2.65 \pm 0.12$. According to the works cited, the concentration range can be divided into several intervals; critical exponent is constant in each such interval within the accuracy of calculations, but differs for different intervals. A step-like universality of the critical exponent is assumed to explain these data for three-dimensional dilute Ising systems. Note that the critical exponent $z(1.0) = 1.98 \pm 0.08$ of the homogeneous system without impurities agrees well with the data found in Ref. [208] by complicated numerical calculations using special coding algorithms. Similar investigations were carried out in Refs [215–219] for the $2d$ Ising model on a simple square lattice with spin concentrations $p = 1.0, 0.95, 0.9, 0.85, 0.80, 0.75, 0.70$ and lattice size $L \times L = 400 \times 400$. At a spin concentration higher than $p \geq 0.9$, the dynamic behavior of the disordered Ising model is shown to belong to the same universality class as that in the homogeneous model with an exponent $z = 2.24 \pm 0.07$. This value agrees well with the data obtained by the field theory [215–219]. Although the accuracy of calculations of the exponent z is not high, the model as well as the procedure used in these works are worthy of notice.

7. Conclusion

In this review, we have made an attempt to consider the results of the study of phase transformations and critical exponents obtained by the Monte Carlo (MC) method in recent years. The method is ideally suited to the study of small-size systems, and in combination with the finite-size scaling theory is effective to investigate ‘macrosystems.’ We

have demonstrated that the MC method is a powerful and versatile tool to study not only classical but also quantum spin systems. It capable of treating complicated models, which can hardly be investigated by other methods, and enables one to calculate critical exponents and critical amplitudes with a high accuracy. We have indicated some works, where the universality class of the critical behavior of certain models is determined from the MC data. We have also presented for these models the critical exponents derived from the MC data treated by the conventional power dependences as well as the finite-size scaling theory. All the data of numerical calculations are compared with the theoretical estimates and experimental evidence.

Unfortunately, the application of the MC method to fields such as spin glasses, ferroelectrics, high-temperature superconductors, liquids, polymers, and many others has remained beyond the scope of this review. The areas of application of the MC method are so wide that all interesting problems of modern physics of phase transformations and critical phenomena, which are not closely related, can hardly be considered in a single review. We believe new highly efficient MC methods specially developed to study the critical region to be of interest and discussed in detail. These and quantum MC methods should to be the goal of a separate review elsewhere.

References

1. Patashinskiĭ A Z, Pokrovskii V L *Fluktuatsionnaya Teoriya Fazovykh Perekhodov* (Fluctuation Theory of Phase Transitions) (Moscow: Nauka, 1982) [Translated into English (Oxford: Pergamon Press, 1979)]
2. Ma Shang-keng *Modern Theory of Critical Phenomena* (London: W.A. Benjamin, Inc., 1976) [Translated into Russian (Moscow: Mir, 1980)]
3. Wilson K G, Kogut J *The Renormalization Group and the ϵ Expansion* (Amsterdam: North-Holland, 1974) [Translated into Russian (Moscow: Mir, 1975)]; *Phys. Rep.* **12** 79 (1974)
4. Stanley H E *Introduction to Phase Transitions and Critical Phenomena* (Oxford: Clarendon Press, 1971) [Translated into Russian (Moscow: Mir, 1973)]
5. Ginzburg V L *Fiz. Tverd. Tela* (Leningrad) **2** 2031 (1960)
6. Le Guillou J J C, Zinn-Justin J *Phys. Rev. B* **21** 3976 (1980)
7. Le Guillou J J C, Zinn-Justin J J. *Phys. Lett.* (Paris) **46** L137 (1985)
8. Antonenko S A, Sokolov A I *Phys. Rev. E* **51** 1894 (1995)
9. Ginzburg V L *O Fizike i Astrofizike* (On Physics and Astrophysics) (Moscow: Nauka, 1985)
10. Binder K (Ed.) *Monte Carlo Methods in Statistical Physics* (Berlin: Springer, 1979) [Translated into Russian (Moscow: Mir, 1982)]
11. Zamalin V M, Norman G Ė, Filinov V S *Metod Monte-Karlo v Statisticheskoi Termodinamike* (Monte Carlo Methods in Statistical Thermodynamics) (Moscow: Nauka, 1977)
12. Binder K, Heerman D *Monte Carlo Simulation in Statistical Physics* (Berlin: Springer-Verlag, 1986) [Translated into Russian (Moscow: Nauka, 1995)]
13. Heerman D *Computer Simulation Methods in Theoretical Physics* (Berlin: Springer-Verlag, 1986) [Translated into Russian (Moscow: Nauka, 1990)]
14. Koonin S E *Computational Physics* (Redwood, Calif.: Addison-Wesley Publ. Co., 1986) [Translated into Russian (Moscow: Mir, 1992)]
15. Binder K, in *Phase Transitions and Critical Phenomena* Vol. 5B (Eds C Domb, M S Green) (New York: Academic, 1976) p. 1
16. Mouritsen O G *Computer Studies of Phase Transitions and Critical Phenomena* (Berlin: Springer, 1984)
17. Landau D P *Physica A* **205** 41 (1994)
18. *Computer Simulation Studies* (Condensed Matter Physics) (Berlin: Springer, 1988)
19. Landau L D, Lifshitz E M *Statisticheskaya Fizika* Chast' 1 (Statistical Physics. Part 1) (Moscow: Nauka, 1976) [Translated into English (Oxford: Pergamon Press, 1980)]
20. Wood W W "Monte Carlo studies of simple liquids", in *Physics of Simple Liquids* (Eds H N V Temperley, J S Rowlinson, G S Rushbrooke) (Amsterdam: North-Holland, 1975) [Translated into Russian (Moscow: Mir, 1978)]
21. Ermakov S M *Metod Monte-Karlo i Smezhnye Voprosy* (Monte Carlo Methods and Related Questions) (Moscow: Nauka, 1975)
22. Metropolis N et al. *J. Chem. Phys.* **21** 1087 (1953)
23. Goodman J, Sokal A D *Phys. Rev. Lett.* **56** 1015 (1986)
24. Goodman J, Sokal A D *Phys. Rev. D* **40** 2035 (1989)
25. Kandel D et al. *Phys. Rev. Lett.* **60** 1591 (1988)
26. Kandel D, Domany E, Brand A *Phys. Rev. B* **40** 330 (1980)
27. Ben-Av R et al. *J. Stat. Phys.* **58** 125 (1990)
28. Kandel D, Ben-Av R, Domany E *Phys. Rev. Lett.* **65** 941 (1990)
29. Creutz M *Phys. Rev. D* **36** 515 (1987)
30. Brown F R, Woch T J *Phys. Rev. Lett.* **58** 2394 (1987)
31. Adler S L *Phys. Rev. D* **38** 1349 (1988)
32. Adler S L *Phys. Rev. D* **23** 2901 (1981)
33. Schmidt K E *Phys. Rev. Lett.* **51** 2175 (1983)
34. Faas M, Hilhorst Y J *Physica A* **135** 571 (1986)
35. Hahn H H, Streit T S J *Physica A* **154** 108 (1988)
36. Stoll E P J. *Phys.: Condens. Matter* **1** 6959 (1989)
37. Swendsen R H, Jang J-S *Phys. Rev. Lett.* **58** 86 (1987)
38. Wolff U *Phys. Rev. Lett.* **62** 361 (1989)
39. Ferrenberg A M, Swendsen R H *Phys. Rev. Lett.* **61** 2635 (1988)
40. Ferrenberg A M, Swendsen R H *Phys. Rev. Lett.* **63** 1195 (1989)
41. Campos P R A, Onody R N *Phys. Rev. B* **56** 14529 (1997)
42. Swendsen R H, Jang J-S *Phys. Rev. Lett.* **57** 2607 (1986)
43. Hokushima K, Nemoto K J. *Phys. Soc. Jpn.* **65** 1604 (1996)
44. Jang J-S, Swendsen R H *Phys. Rev. B* **38** 4840 (1988)
45. Jang J-S, Swendsen R H *Phys. Rev. B* **38** 9086 (1988)
46. Klein W, Ray T, Tamayo P *Phys. Rev. Lett.* **62** 163 (1989)
47. Suzuki M *Prog. Theor. Phys.* **56** 1454 (1976)
48. Suzuki M *Prog. Theor. Phys.* **58** 1377 (1977)
49. De Raedt H, Lagendijk A *Phys. Rev. Lett.* **46** 77 (1981)
50. Hirsch I E et al. *Phys. Rev. Lett.* **47** 1628 (1981)
51. De Raedt H, Lagendijk A *Phys. Rep.* **127** 233 (1985)
52. Fay R M *Phys. Rev. B* **33** 6271 (1986)
53. Wiessler A *Phys. Lett. A* **82** 359 (1982)
54. Novotny M A, Landau D P *Bull. Am. Phys. Soc.* **24** 361 (1979)
55. Cullen I I, Landau D P *Bull. Am. Phys. Soc.* **26** 576 (1981)
56. Elesin V F, Kashurnikov V A *Zh. Eksp. Teor. Fiz.* **106** 1773 (1994) [*JETP* **79** 961 (1994)]
57. Berkov D V, Meshkov S V *Pis'ma Zh. Eksp. Teor. Fiz.* **52** 1021 (1990) [*JETP Lett.* **52** 415 (1990)]
58. Kashurnikov V A *Zh. Eksp. Teor. Fiz.* **108** 1796 (1995) [*JETP* **81** 984 (1995)]
59. Kashurnikov V A *Phys. Rev. B* **53** 5932 (1996)
60. Kashurnikov V A, Kharchenko Yu G *Pis'ma Zh. Eksp. Teor. Fiz.* **63** 860 (1996) [*JETP Lett.* **63** 900 (1996)]
61. Kashurnikov V A, Krasavin A V, Svistunov B V *Pis'ma Zh. Eksp. Teor. Fiz.* **64** 92 (1996) [*JETP Lett.* **64** 99 (1996)]
62. Lubartsev A P, Vorontsov-Velyaminov P N *Phys. Rev. A* **48** 4075 (1993)
63. Aplesnin S S *Fiz. Tverd. Tela* **38** 1868 (1996)
64. Aplesnin S S *Fiz. Tverd. Tela* **39** 1404 (1997)
65. Aplesnin S S *Phys. Low-Dim. Struct.* (10) 95 (1997)
66. Evertz H G, Lana G, Mareu M *Phys. Rev. Lett.* **70** 875 (1993)
67. Sandvik A W, Kurkijarvi J *Phys. Rev. B* **43** 5950 (1991)
68. Sandvik A W *J. Phys. A* **25** 3667 (1992)
69. Beard B B, Wiese V J *Phys. Rev. Lett.* **77** 5130 (1996)
70. Prokof'ev N V, Svistunov B V, Tupitsyn I S *Pis'ma Zh. Eksp. Teor. Fiz.* **64** 853 (1996) [*JETP Lett.* **64** 911 (1996)]
71. Prokof'ev N V, Svistunov B V, Tupitsyn I S *Zh. Eksp. Teor. Fiz.* **114** 570 (1998) [*JETP* **87** 310 (1998)]
72. Handscomb D C *Proc. Camb. Phys. Soc.* **58** 594 (1962)
73. Handscomb D C *Proc. Camb. Phys. Soc.* **60** 115 (1964)
74. Lyklema I W *Phys. Rev. Lett.* **49** 88 (1982)
75. Lyklema I W *Phys. Rev. B* **27** 3108 (1983)
76. Lee D H, Joannopoulos I D, Negele I W *Phys. Rev. B* **30** 1599 (1984)

77. Gomes-Santos G, Joannopoulos I D, Negele I W *Phys. Rev. B* **39** 4435 (1989)
78. Monousakis E, Salvador R *Phys. Rev. B* **39** 575 (1989)
79. Chakravarty S C, Stein D B *Phys. Rev. Lett.* **49** 582 (1982)
80. Favorskii I A, Gutman A G, Rozhdestvenskii I V *Kristallografiya* **30** 1050 (1985)
81. Rozhdestvenskii I A, Murtazaev A K, Favorskii I A, Preprint ITF AN UkrSSR, No. ITF-87-158R (Kiev: ITF AN UkrSSR, 1987)
82. Favorskii I A et al. Preprint ITF AN UkrSSR, No. ITF-85-94R (Kiev: ITF AN UkrSSR, 1985)
83. Murtazaev A K, Favorskii I A *Fiz. Nizk. Temp.* **18** 144 (1992)
84. Murtazaev A K, PhD Thesis (Leningrad: LGU, 1987)
85. Favorsky I A, Kuznetsova T N, Vorontsov-Velyaminov P N *J. Phys.: Condens. Matter* **4** 2629 (1992)
86. Kuznetsova T V, Vorontsov-Velyaminov P N *J. Phys.: Condens. Matter* **5** 717 (1993)
87. Rozdestvensky I V, Favorsky I A *Molecular Simulation* **9** 213 (1992)
88. *Monte Carlo Methods in Quantum Problems* (NATO ASI Series. Ser. C, no 125, Ed. M H Kalos) (Dordrecht: Kluwer Academic, 1984)
89. Kawashima N, Gubernatis I E *Phys. Rev. Lett.* **73** 1295 (1994)
90. Neirotti I P, de Olivera M I *Phys. Rev. B* **53** 668 (1996)
91. Landau D P *Phys. Rev. B* **13** 2997 (1976)
92. Landau D P *Phys. Rev. B* **14** 255 (1976)
93. Landau D P *Phys. Rev. B* **16** 4164 (1977)
94. Binder K Z *Phys. B* **43** 119 (1981)
95. Binder K *Phys. Rev. Lett.* **47** 693 (1981)
96. Barber M N, in *Phase Transitions and Critical Phenomena* Vol. 8 (Eds C Domb, J L Lebowitz) (New York: Academic, 1983) p. 1
97. Landau D P, Binder K *Phys. Rev. B* **31** 5946 (1985)
98. Binder K, Landau D P *Phys. Rev. Lett.* **52** 318 (1984)
99. Peczak P, Landau D P *Phys. Rev. B* **39** 11932 (1989)
100. Landau D P *J. Magn. Magn. Mater.* **31–34** 11 (1983)
101. Bhatt R N, Yang A P *Phys. Rev. Lett.* **54** 424 (1985)
102. Bidaux R, Boccardo N *Phys. Rev. B* **34** 4881 (1986)
103. Danino M *Solid State Commun.* **52** 885 (1984)
104. Rieqo H, Young A P *J. Phys. A* **26** 5279 (1993)
105. Gawlimski E T et al. *Phys. Rev. B* **32** 1575 (1985)
106. Andelman D *Phys. Rev. B* **34** 6214 (1986)
107. Newman M E J, Barkema G T *Phys. Rev. E* **53** 393 (1996)
108. Aoyma Y, Chen W, Tanaka M *J. Phys. Soc. Jpn.* **66** 272 (1997)
109. Nagai O et al. *Phys. Rev. B* **35** 3425 (1987)
110. Dekker C, Dikken B J, Arts A F M *Solid State Commun.* **54** 887 (1985)
111. Neda Z *J. Phys. Soc. I* **4** 175 (1994)
112. Hau Lu, Ticke J W *J. Magn. Magn. Mater.* **140–144** 1509 (1996)
113. Coppersmith S N *Phys. Rev. B* **32** 1584 (1985)
114. Kimel J D et al. *Phys. Rev. B* **35** 3347 (1987)
115. Kerler W, Rehberg P *Phys. Rev. B* **49** 9688 (1994)
116. Binder K, Landau D P *Phys. Rev. B* **21** 1941 (1980)
117. Oitmaa J, Fernander J F *Phys. Rev. B* **39** 11920 (1989)
118. Hernandez L, Cero H *Phys. Rev. B* **43** 698 (1991)
119. Ledue D, Landau D P, Teillet J *Phys. Rev. B* **51** 12523 (1995)
120. Janke W, Katoot M, Villanova R *Phys. Rev. B* **49** 9644 (1994)
121. Fernandez J F et al. *Phys. Rev. B* **27** 4274 (1983)
122. Gualin B D, Collins M F *Phys. Rev. B* **33** 6287 (1986)
123. Serena P A et al. *Phys. Rev. B* **47** 5027 (1993)
124. Hurcht A, Moschel A, Usadel K D *J. Magn. Magn. Mater.* **148** 32 (1995)
125. Chen K, Ferrenberg A M, Landau D P *J. Appl. Phys.* **73** 5488 (1993)
126. Rozhdestvenskii I A, Murtazaev A K, Favorskii I A, Preprint ITF AN UkrSSR, No. ITF-87-158R (Kiev: ITF AN UkrSSR, 1987)
127. Mailhot A, Plumer M L, Caille A *J. Appl. Phys.* **67** 5418 (1990)
128. Peczak P, Ferrenberg A M, Landau D P *Phys. Rev. B* **43** 6087 (1991)
129. Murtazaev A K *Mat. Model.* **4** 114 (1992)
130. Challa M S S, Landau D R, Binder K *Phys. Rev. B* **34** 1841 (1986)
131. Alves N A, Berg B A, Villanova R *Phys. Rev. B* **43** 5846 (1991)
132. Chen J-A, Hu Ch-K *Phys. Rev. B* **50** 6220 (1994)
133. Zhang G-H, Yang Ch-Zh *J. Phys. A* **26** 4907 (1993)
134. Marcu M, Muller J *Phys. Lett. A* **119** 469 (1987)
135. Mason T E, Collins M F, Gaulin B D *J. Appl. Phys.* **67** 5421 (1990)
136. Harrison A, Mason T E *J. Appl. Phys.* **67** 5424 (1990)
137. Rumirez-Santiago G, Jose J V *Phys. Rev. B* **49** 9567 (1994)
138. Pires A S T, Pereira A R, Gouvea M E *Phys. Rev. B* **49** 9663 (1994)
139. Vismanath V S et al. *Phys. Rev. B* **49** 9702 (1994)
140. Derchko O, Krokhmalkskii T *J. Magn. Magn. Mater.* **140–144** 1623 (1995)
141. Cuccoli A, Tognetti V *Phys. Rev. B* **52** 10221 (1995)
142. Li W-Z, Zhang J-B *Phys. Lett. B* **200** 125 (1988)
143. Stuben H, Hege H-C, Nakamura A *Phys. Lett. B* **244** 473 (1990)
144. Zhang J-B, Ji D-R *Phys. Lett. B* **151** 469 (1990)
145. Espriu D et al. *Nucl. Phys. B* **265** 92 (1986)
146. Ferrenberg A M, Landau D P *Phys. Rev. B* **44** 5081 (1991)
147. Chen K, Ferrenberg A M, Landau D P *Phys. Rev. B* **48** 3249 (1993)
148. Holm Ch, Janke W *Phys. Rev. B* **48** 936 (1993)
149. Mailhot A, Plumer M L, Caille A *Phys. Rev. B* **50** 6854 (1994)
150. Kawamura H *J. Phys. Soc. Jpn.* **56** 474 (1986)
151. Kawamura H *J. Phys. Soc. Jpn.* **61** 1299 (1992)
152. Nijmeijer M J P, Weis J J *Phys. Rev. E* **53** 591 (1996)
153. Schlottmann P *Phys. Rev. B* **33** 4880 (1986)
154. Adler J, Oitmaa J *J. Phys. C* **12** 575 (1979)
155. Nagaev É L *Usp. Fiz. Nauk* **136** 61 (1982) [*Sov. Phys. Usp.* **25** 31 (1982)]
156. Roger M, Hetherington J H, Delrien J M *Rev. Mod. Phys.* **55** 1 (1983)
157. Rushbrooke G S, Baker G A, Wood P J, in *Phase Transitions and Critical Phenomena* (Eds C Domb, M S Green) (New York: Academic Press, 1974)
158. Raedt H, Lagendijk A *Phys. Rep.* **127** 233 (1985)
159. Aplesnin S S *Fiz. Tverd. Tela* (S.-Peterburg) **37** 1307 (1995)
160. Murtazaev A K, Favorskii I A *Fiz. Nizk. Temp.* **19** 160 (1993)
161. Murtazaev A K, Khizriev K Sh, Kamilov I K, Aliev Kh K *Mat. Model.* **9** 36 (1997)
162. Favorskii I A et al., Preprint ITF AN UkrSSR: No. ITF-85-93R (Kiev: ITF AN UkrSSR, 1985)
163. Murtazaev A K, Favorskii I A *Vestn. Leningr. Univ. Ser. 4* (3) 18 (1987)
164. Morokhov I D et al. *Usp. Fiz. Nauk* **133** 653 (1981) [*Sov. Phys. Usp.* **24** 295 (1981)]
165. Petrov Yu I *Fizika Malykh Chastits* (Physics of Small Particles) (Moscow: Nauka, 1982)
166. Morokhov I D, Trusov L I, Lapovok V N *Fizicheskie Yavleniya v Ul'tradispersnykh Sredakh* (Physical Phenomena in Ultradisperse Media) (Moscow: Energoatomizdat, 1984)
167. Nepiiko S A *Fizicheskie Svoistva Malykh Metallicheskich Chastits* (Physical Properties of Small Metal Particles) (Kiev: Naukova Dumka, 1985)
168. Petrov Yu I *Klastery i Malye Chastitsy* (Clusters and Small Particles) (Moscow: Nauka, 1986)
169. Halperin W P *Rev. Mod. Phys.* **58** 533 (1986)
170. Smirnov B M *Usp. Fiz. Nauk* **162** (1) 119 (1992) [*Sov. Phys. Usp.* **35** 37 (1992)]
171. Nagaev É L *Usp. Fiz. Nauk* **162** (9) 47 (1992) [*Sov. Phys. Usp.* **35** 747 (1992)]
172. Dobrovitskii V V, Zvezdin A K, Popkov A F *Usp. Fiz. Nauk* **166** 439 (1996) [*Phys. Usp.* **39** 407 (1996)]
173. Gusev A I *Usp. Fiz. Nauk* **168** 55 (1998) [*Phys. Usp.* **41** 49 (1998)]
174. Zvezdin A K, Popov A I *Zh. Eksp. Teor. Fiz.* **109** 2115 (1996) [*JETP* **82** 1140 (1996)]
175. Zvezdin A K et al. *Zh. Eksp. Teor. Fiz.* **109** 1742 (1996) [*JETP* **82** 939 (1996)]
176. Dobrovitski V V, Zvezdin A K *Europhys. Lett.* **38** 377 (1997)
177. Mukhin A A, Saiko G V, Zvezdin A K, Preprint IOF RAN No. 9 (Moscow: IOF RAN, 1994)
178. Kadomtsev B B *Dinamika i Informatsiya* (Dynamics and Information) (Moscow: Red. Zh. Usp. Fiz. Nauk, 1997)
179. Andreev A F *Usp. Fiz. Nauk* **168** 655 (1998) [*Phys. Usp.* **41** 581 (1998)]
180. Zvezdin A K et al. *Usp. Fiz. Nauk* **168** 1141 (1998) [*Phys. Usp.* **41** 1037 (1998)]
181. Samuelsen E J, Hutchings M T, Shirane G *Physica* **48** 13 (1970)
182. Altman J O, Murphy J C, Fones S *Phys. Rev. A* **38** 912 (1988)
183. Foner S *Phys. Rev.* **130** 183 (1963)
184. Binder K, Hoenberg P C *Phys. Rev. B* **9** 2194 (1974)
185. Murtazaev A K et al. *Fiz. Nizk. Temp.* **24** 462 (1998)
186. Murtazaev A K et al. *Fiz. Tverd. Tela* **40** 1661 (1998)

187. Murtazaev A K et al. *Proceedings of 5th ATPC'98* (Seoul, Korea, 1998) p. 109
188. Bednars G, Geldart D J W, White M A *Phys. Rev. B* **47** 14247 (1993)
189. Marinelli M et al. *Phys. Rev. B* **49** 9523 (1994)
190. Bruce R H, Cannel D S *Phys. Rev. B* **15** 4451 (1977)
191. Kamilov I K, Aliev Kh K *Statisticheskie Kriticheskie Yavleniya v Magnitouporyadochennykh Kristallakh* (Statistical Phenomena in Magnetic Ordered Crystals) (Makhachkala: Izd. DNTs RAN, 1993)
192. Dormann L J, Fiorani D, Trone E *Adv. Chem. Phys.* **98** 283 (1997)
193. Hendriksen P V, Linderöth S, Lindgard P-A *Phys. Rev B* **48** 7259 (1993)
194. Fisher E, Gorodetsky G, Shtrikman J. *Phys. Colloq.* (Paris) **32** 1 (1971)
195. Ferdinand A E, Fisher M E *Phys. Rev.* **185** 832 (1969)
196. Fisher M E, Barber M N *Phys. Rev. Lett.* **28** 1516 (1972)
197. Paauw Th T A, Compagner A, Bedeaux D *Physica A* **79** 1 (1975)
198. Halperin B I, Hohenberg P C *Phys. Rev.* **177** 952 (1969)
199. Hohenberg P C, Halperin B C *Rev. Mod. Phys.* **49** 435 (1977)
200. Maleev S V, Preprint LIYaF AN SSSR No. 1038 (Leningrad, LIYaF, 1985)
201. Maleev S V, Preprint LIYaF AN SSSR No. 1039 (Leningrad, LIYaF, 1985)
202. Maleev S V, Preprint LIYaF AN SSSR No. 1039 (Leningrad: LIYaF, 1985)
203. Kamilov I K, Aliev Kh K *Usp. Fiz. Nauk* **168** 953 (1998) [*Phys. Usp.* **41** 865 (1998)]
204. Teitel'baum G B *Pis'ma Zh. Eksp. Teor. Fiz.* **21** 339 (1975) [*JETP Lett.* **21** 154 (1975)]
205. Miyashita S, Takano H *Prog. Theor. Phys.* **73** 1122 (1985)
206. Demenev A G *Mat. Model.* **8** 47 (1996)
207. Wansleben S, Landau D P *J. Appl. Phys.* **61** 3968 (1987)
208. Wansleben S, Landau D P *Phys. Rev. B* **43** 6006 (1991)
209. O'Onario De Meo, Reger J D, Binder K *Physica A* **220** 628 (1995)
210. Landau D P, Chen K, Bunker A J. *Magn. Magn. Mater.* **140–144** 1473 (1995)
211. Peczak P, Landau D P *Phys. Rev. B* **47** 14260 (1993)
212. Grandi B C J, Figueiredo W *Phys. Rev. E* **54** 4722 (1996)
213. Vakilov A N, Prudnikov V V *Pis'ma Zh. Eksp. Teor. Fiz.* **55** 709 (1992) [*JETP Lett.* **55** 741 (1992)]
214. Prudnikov V V, Vakilov A N *Zh. Eksp. Teor. Fiz.* **103** 962 (1993) [*Sov. Phys. JETP* **76** 469 (1993)]
215. Markov O N, Prudnikov V V *Izv. Vyssh. Uchebn. Zaved. Ser. Fiz.* **37** (8) 83 (1994)
216. Markov O N, Prudnikov V V *Pis'ma Zh. Eksp. Teor. Fiz.* **60** (1–2) 24 (1994) [*JETP Lett.* **60** 23 (1994)]
217. Prudnikov V V, Markov O N *Europhys. Lett.* **29** 245 (1995)
218. Prudnikov V V, Markov O N *J. Phys. A* **28** 1549 (1995)
219. Markov O N, Prudnikov V V *Fiz. Tverd. Tela* **37** 1574 (1995)
220. Prudnikov V V et al. *Zh. Eksp. Teor. Fiz.* **114** (3) 972 (1998) [*JETP* **87** 527 (1998)]
221. Marz R, Hunter D, Jan N *J. Stat. Phys.* **74** 903 (1994)
222. Chakrabarti C K, Baumgartel H G, Stauffer D *Z. Phys.* **44** 333 (1981)
223. Yalabik M C, Gunton J D *Phys. Rev. B* **25** 534 (1982)
224. Jan N, Mosley L L, Stauffer D *J. Stat. Phys.* **33** 1 (1983)
225. Kalle C J. *Phys. A* **17** L801 (1984)
226. Pearson R B, Richardson J L, Touissaint D *Phys. Rev. B* **31** 4472 (1985)
227. Bausch R et al. *Phys. Rev. Lett.* **47** 1837 (1981)
228. Bhanot J, Duke D, Salvador R *Phys. Rev. B* **33** 7841 (1986)
229. Abe R *Prog. Theor. Phys.* **39** 947 (1986)
230. Suzuki M *Prog. Theor. Phys.* **58** 1142 (1977)
231. Halperin B I, Hohenberg P C, Ma S-K *Phys. Rev. B* **10** 139 (1974)
232. Suzuki M *Prog. Theor. Phys.* **50** 1767 (1973)
233. De Dominicis C, Brezin E, Zinn-Justin J *Phys. Rev. B* **12** 4945 (1975)
234. Landau L D, Khalatnikov I V *Dokl. Akad. Nauk SSSR* **96** 469 (1954)
235. Van Hove L *Phys. Rev.* **93** 1374 (1954)
236. Harris A B *J. Phys. C* **7** 1671 (1974)
237. Khmel'nitskiĭ D E *Zh. Eksp. Teor. Fiz.* **68** 1960 (1975) [*Sov. Phys. JETP* **41** 981 (1975)]
238. Grinstein G, Ma S-K, Mazenko G F *Phys. Rev. B* **15** 258 (1977)